

Journal Pre-proof

Discovery, structure-activity relationship study and biological evaluation of 2-thioureidothiophene-3-carboxylates as a novel class of C-X-C chemokine receptor 2 (CXCR2) antagonists

Ding Xue, Wenmin Chen, Nouri Neamati



PII: S0223-5234(20)30357-3

DOI: <https://doi.org/10.1016/j.ejmech.2020.112387>

Reference: EJMECH 112387

To appear in: *European Journal of Medicinal Chemistry*

Received Date: 10 February 2020

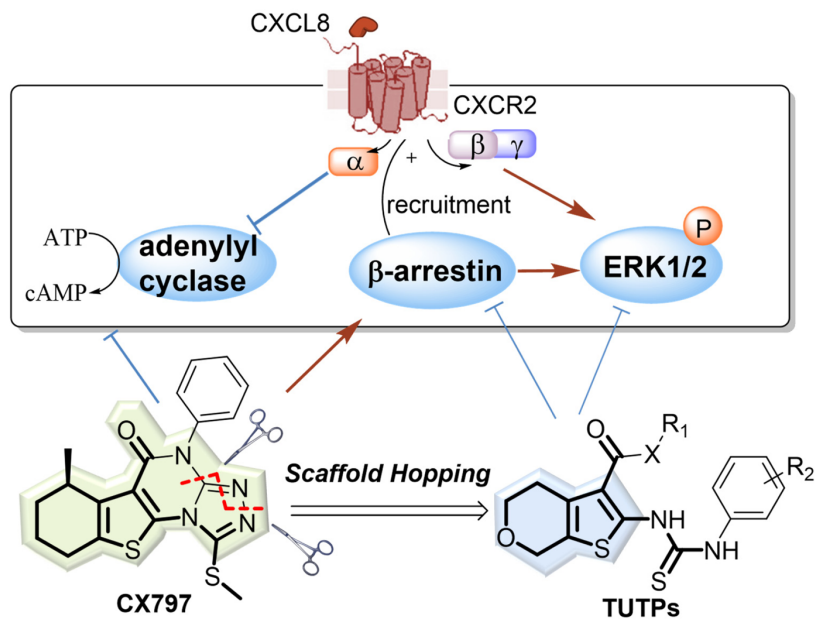
Revised Date: 9 April 2020

Accepted Date: 23 April 2020

Please cite this article as: D. Xue, W. Chen, N. Neamati, Discovery, structure-activity relationship study and biological evaluation of 2-thioureidothiophene-3-carboxylates as a novel class of C-X-C chemokine receptor 2 (CXCR2) antagonists, *European Journal of Medicinal Chemistry*, <https://doi.org/10.1016/j.ejmech.2020.112387>.

This is a PDF file of an article that has undergone enhancements after acceptance, such as the addition of a cover page and metadata, and formatting for readability, but it is not yet the definitive version of record. This version will undergo additional copyediting, typesetting and review before it is published in its final form, but we are providing this version to give early visibility of the article. Please note that, during the production process, errors may be discovered which could affect the content, and all legal disclaimers that apply to the journal pertain.

© 2020 Published by Elsevier Masson SAS.



Discovery, Structure-Activity Relationship Study and Biological Evaluation of 2-Thioureidothiophene-3-carboxylates as a Novel Class of C-X-C Chemokine Receptor 2 (CXCR2) Antagonists

Ding Xue,^{†,▽} Wenmin Chen,^{†,▽} and Nouri Neamati^{*,†}

[†]Department of Medicinal Chemistry, College of Pharmacy, Rogel Cancer Center, University of Michigan, North Campus Research Complex, 1600 Huron Parkway, Ann Arbor, Michigan, 48109, United States.

ABSTRACT

The C-X-C motif ligand 8 and C-X-C chemokine receptor 2 (CXCL8-CXCR2) axis is involved in pathogenesis of various diseases including inflammation and cancers. Various CXCR2 antagonists are under development for several diseases. Our previous high-throughput cell-based assay specific for CXCR2 has identified a pyrimidine-based compound CX797 acting on CXCR2 down-stream signaling. A lead optimization campaign through scaffold-hopping strategy led to a series of 2-thioureidothiophene-3-carboxylates (TUTP) as novel CXCR2 antagonists. Structure-activity relationship study of TUTPs led to the identification of compound **52** that significantly inhibited CXCR2-mediated β -arrestin recruitment signaling ($IC_{50} = 1.1 \pm 0.01 \mu M$) with negligible effect on CXCL8-mediated cAMP signaling and calcium flux. Similar to the known CXCR2 antagonist SB265610, compound **52** inhibited CXCL8-CXCR2 induced phosphorylation of ERK1/2. TUTP compounds also inhibited CXCL8-mediated cell

migration and showed synergy with doxorubicin in ovarian cancer cells, thereby supporting TUTPs as promising compounds for cancer treatment.

KEYWORDS

CXCR2; Thioureidothiophene; β -arrestin; GPCR; CXCL8; cAMP;

INTRODUCTION

CXCR2 is a member of the seven transmembrane G-protein-coupled receptor (GPCR) family expressed on immune cells, endothelial cells, epithelial cells, as well as various types of cancer cells.¹ CXCR2 mediates its downstream biological effects upon binding with high affinity to CXCL8 as well as other ELR⁺ (Glu4-Leu5-Arg6)-containing chemokines including CXCL1, 2, 3, 5, 6 and 7.²

The CXCL8-CXCR2 axis is involved in the pathogenesis of various diseases including inflammation and cancers. As the first and most intensively studied chemokine, CXCL8 plays an essential role in the recruitment and migration of neutrophils during inflammatory process, thus the modulation of this pathway is beneficial in the treatment of various diseases including chronic obstructive pulmonary disorder (COPD), asthma, cystic fibrosis and arthritis.³ The secretion of CXCL8 and its activation of CXCR2 are also increasingly recognized as key factors for tumor growth, invasion, angiogenesis and metastasis. CXCR2 signaling is important for the microenvironment of select tumor types and has a regulatory effect on cancer stem cells proliferation and self-renewal.^{2,4} While overexpression of CXCL8 is associated with several late stage diseases, CXCR2 expression level is correlated with prognosis and therapeutic outcome of patients with colorectal cancer,⁵ bladder cancer,⁶ hepatocellular carcinoma⁷ and laryngeal

squamous cell carcinoma.⁸ Upregulation of CXCR2 in resistant cancer cell lines also indicates its involvement in the development of resistance to chemotherapies.⁹⁻¹¹ The multiple effects of CXCL8 signaling within the tumor pathology suggest that the targeting of CXCL8-CXCR2 may have important implications to halt cancer progression and to sensitize tumor cells to chemotherapies.

Given the importance of CXCR2 signaling pathway in inflammatory disorders and cancers, the antagonists of CXCR2 have received increasing attention over the past twenty years.¹²⁻¹⁶ Since the discovery of the first small-molecule CXCR2 antagonists in 1998,¹⁷ a number of CXCR2 antagonists have been developed and at least nine of them have advanced to clinical stage for COPD, asthma, arthritis and cancer treatments (Figure. 1). Diarylureas SB656933 and danirixin were tested in Phase I and II clinical trial respectively for the treatment of COPD.¹⁸⁻²⁰ The bioisosteric replacement of the urea led to the development of another series of CXCR2 antagonists with a squaramide core. Navarixin from this class exhibited significant anti-tumor activity in melanoma and colon cancer mouse models,^{21,22} and it is now under Phase II clinical trial.²³ Several other antagonists with distinct structure motifs are also under clinical development for the treatment of cancer and inflammatory diseases. Repertaxin is tested as single agent or in combination for the treatment of breast cancer or symptoms associated with organ transplantations.²⁴ AZD8309, AZD5069 and AZD4721 are a series of 2-(benzylthio)pyrimidines that have been testing for nasal inflammation, COPD, asthma, and prostate cancer.²⁵ SX-682 is another close analog with a distinct boronic acid group that enhance T cell activation and antitumor immunity and is now tested in combination with pembrolizumab in Phase I/II trial for metastatic melanoma.^{26,27}

Since the crystal structure of CXCR2 has not yet been solved, ligand-based drug design and high-throughput screening are the most feasible approaches for discovery of CXCR2 antagonists. We previously discovered a novel pyrimidine-based compound CX797 as a potent CXCR2 signaling modulator through a high-throughput screening of our in-house compound library. CX797 inhibits CXCL8 mediated cAMP signaling ($IC_{50} = 7.79 \pm 0.15 \mu\text{M}$), receptor degradation as well as cell migration, while stimulates CXCL8-mediated β -arrestin recruitment.²⁸ CX797 has a planar polycyclic structure and relatively high lipophilicity, which could be detrimental to its drug-like properties like metabolic stability, bioavailability, and hERG binding induced toxicity.^{29, 30} Using the scaffold-hopping strategy, we opened the fused polycyclic ring system of CX797 to produce a series of compounds with thiourea and carboxylate moieties (Figure 2). These compounds, namely 2-thioureidothiophene-3-carboxylates, proved to be a novel class of CXCR2 antagonists and exhibited a distinct profile in the CXCR2 inhibition assay. An extensive SAR study was carried out and the detailed mechanism of action regarding the CXCL8/CXCR2 signaling is presented. Its inhibition of CXCL8-mediated cell migration and the synergistic effect with doxorubicin further warrants its development for treating cancers.

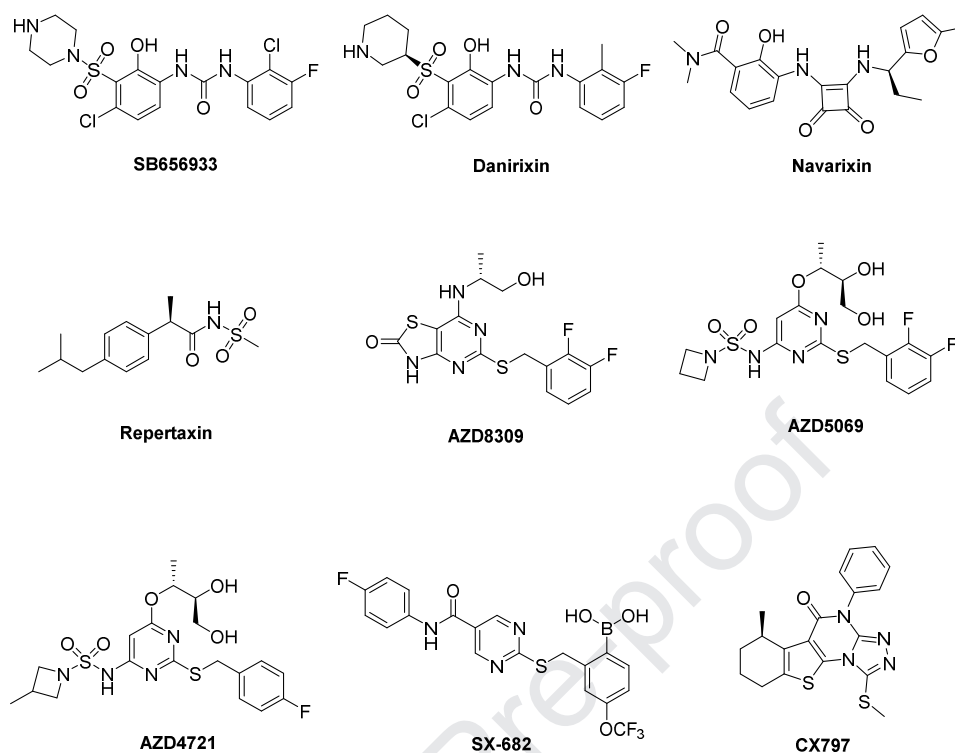


Figure 1. Structures of representative CXCR2 antagonists

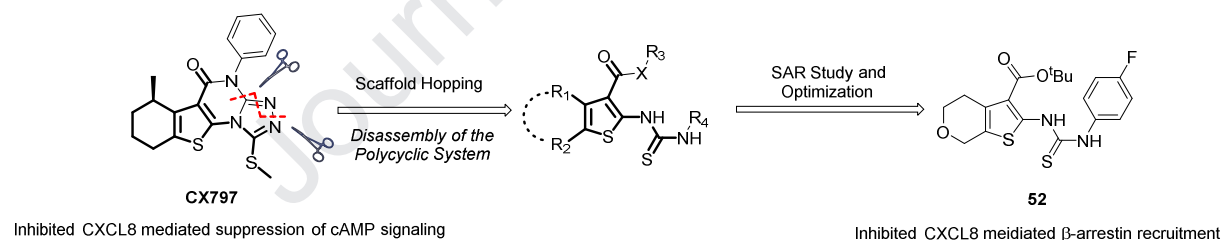


Figure 2. Modification of CX797 using a scaffold-hopping approach

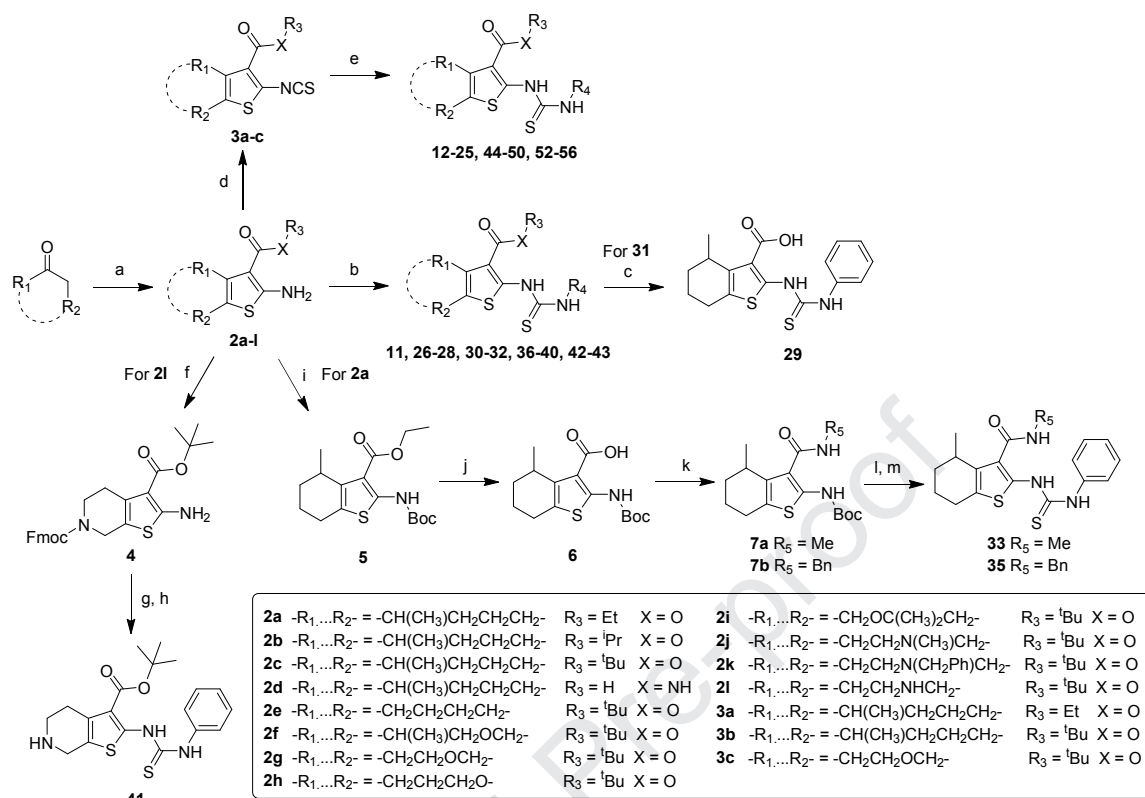
RESULTS AND DISCUSSION

Chemistry

As depicted in Scheme 1, the synthesis of the 2-thioureidothiophene-3-carboxylates and carboxamides derivatives started with a one-pot Gewald reaction employing cyclic ketones, 2-cyanoacetates/2-cyanoacetamide, sulfur and morpholine as starting materials, leading to the

generation of 2-aminothiophene-3-carboxylates/carboxamide **2a-l**. Compared to the standard heated conditions in MeOH, EtOH, or DMF at 50-80 °C,³¹⁻³³ neat condition under room temperature provided improved yields of **2** (average yields 65% versus 31%). Compound **2** was then treated with the appropriate isothiocyanates to afford **11**, **26-28**, **30-32**, **36-40**, **42** and **43**. Compound **29** was obtained through hydrolysis of the *tert*-butyl ester of **31** by TFA. To facilitate the modification on R₄ of the final compounds, **2** was converted into isothiocyanate derivative **3** that was reacted with various anilines/benzyl amines to yield **12-25**, **44-50** and **52-56**. To synthesize compound **41**, intermediate **21** was selectively protected with Fmoc on the piperidine moiety and then reacted with phenyl isothiocyanate, followed by the deprotection of piperidine in DMF. Amides **33** and **35** were synthesized by a different scheme starting from the Boc protection of the 2-amino group of **2a** to give **5**, of which the ethyl ester was hydrolyzed in the presence of NaOH under 80 °C to give **6**. Compound **6** was then coupled with methyl amine or benzylamine in the presence of HATU and DIEA. The resulting compound **7a** and **7b** were deprotected and subsequently reacted with phenyl isothiocyanate to give the final compounds **33** and **35**, respectively (Scheme 1).

Scheme 1. Synthesis of 2-Thioureidothiophene-3-carboxylate Derivatives^a



11-28 -R₁...R₂- = -CH(CH₃)CH₂CH₂CH₂- R₃ = Et X = O

11 R₄ = Ph
12 R₄ = 4-F-Ph
13 R₄ = 4-OMe-Ph
14 R₄ = 4-OCF₃-Ph
15 R₄ = 4-NMe₂-Ph
16 R₄ = 4-^tBu-Ph
17 R₄ = 2,2-difluorobenzo[d][1,3]dioxole-5-yl
18 R₄ = 3,4-di-OMe-Ph
19 R₄ = 4-CF₃-Ph

20 R₄ = 4-NH₂-Ph
21 R₄ = 4-OH-Ph
22 R₄ = 2-OH-Ph
23 R₄ = 2-F-Ph
24 R₄ = 3-OMe-Ph
25 R₄ = Bn
26 R₄ = pyrazine
27 R₄ = benzoyl
28 R₄ = -C(=O)OEt

30-32 -R₁...R₂- = -CH(CH₃)CH₂CH₂CH₂- R₄ = Ph

30 R₃ = ⁱPr X = O
31 R₃ = ^tBu X = O
32 R₃ = H X = NH

36-40, 42, 43 R₃ = ^tBu R₄ = Ph X = O

36 -R₁...R₂- = -CH₂CH₂CH₂CH₂-
37 -R₁...R₂- = -CH(CH₃)CH₂OCH₂-
38 -R₁...R₂- = -CH₂CH₂OCH₂-
39 -R₁...R₂- = -CH₂CH₂CH₂O-
40 -R₁...R₂- = -CH₂OC(CH₃)₂CH₂-
42 -R₁...R₂- = -CH₂CH₂N(CH₃)CH₂-
43 -R₁...R₂- = -CH₂CH₂N(CH₂Ph)CH₂-

44-50 -R₁...R₂- = -CH(CH₃)CH₂CH₂CH₂- R₃ = ^tBu X = O

44 R₄ = 3-OMe-Ph
45 R₄ = 4-OCF₃-Ph
46 R₄ = 4-^tBu-Ph
47 R₄ = 4-OPh-Ph
48 R₄ = 4-(4-methylpiperazin-1-yl)-Ph
49 R₄ = 3,4-di-OMe-Ph
50 R₄ = 2,2-difluorobenzo[d][1,3]dioxole-5-yl

52-56 -R₁...R₂- = -CH₂CH₂OCH₂- R₃ = ^tBu X = O

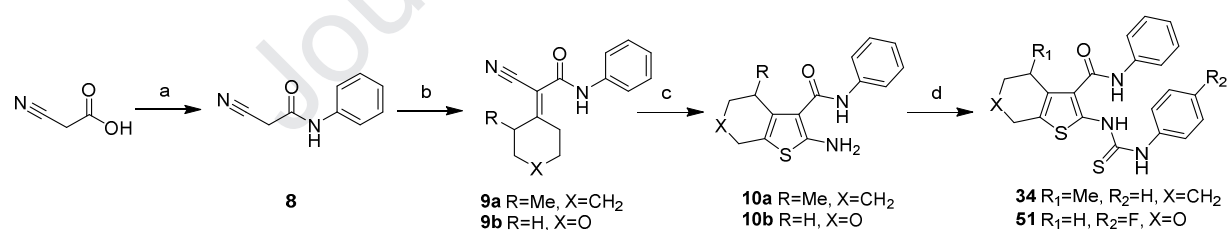
52 R₄ = 4-F-Ph
53 R₄ = 4-OCF₃-Ph
54 R₄ = 3,4-di-OMe-Ph
55 R₄ = (S)-1-phenylethan-1-yl
56 R₄ = (R)-1-phenylethan-1-yl

^a Reagents and conditions: (a) 2-cyanoacetates or 2-cyanoacetamide, sulfur, morpholine, rt; (b) isothiocyanates, pyridine, 60 °C; (c) TFA, DCM, rt; (d) thiophosgene, CaCO₃, DCM, H₂O, rt; (e) amines, pyridine, 60 °C; (f) Fmoc-Cl, Na₂CO₃, dioxane, H₂O, rt; (g) phenyl isothiocyanate, pyridine, 60 °C; (h) piperidine, DMF, rt; (i) (Boc)₂O, DMAP, dioxane, rt; (j) NaOH, THF,

MeOH, H₂O, 80 °C; (k) amines, HATU, DIEA, DMF, rt; (l) HCl, dioxane, rt; (m) phenyl isothiocyanate, pyridine, 60 °C.

A different scheme was applied to the synthesis of amides **34** and **51** (Scheme 2). 2-cyano-*N*-phenylacetamide **8** was obtained by the reaction of 2-cyanoacetic acid with aniline in the presence of EDCI and HOBt. The Gewald reaction as described above was not applicable to amide **8**, and thus a two-step procedure involving the olefin intermediate **9** was employed.³⁴ Compound **8** was treated with 2-methylcyclohexanone or tetrahydro-4*H*-pyran-4-one in the presence of NH₄OAc in AcOH and toluene at 80 °C, providing **9a** (mixture of *Z*- and *E*- isomers) and **9b**, respectively. **9a/9b** was subjected to the cyclization condition to give **10a/10b** in the presence of sulfur and morpholine. For **9a**, only the *Z*-isomer was reacted. **10a/10b** was then heated with phenyl isothiocyanate in pyridine to give **34** and **51**.

Scheme 2. Synthesis of compound **34** and **51**^a

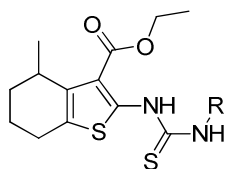


^aReagents and conditions: (a) aniline, EDCI, HOBt, Et₃N, DMF, rt; (b) 2-methylcyclohexanone (for **9a**) or tetrahydro-4*H*-pyran-4-one (for **9b**), NH₄OAc, AcOH, toluene, 80 °C; (c) sulfur, morpholine, EtOH, 60 °C; (d) phenyl isothiocyanate (for **34**) or 4-fluorophenyl isothiocyanate (for **51**), pyridine, 50 °C.

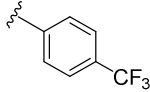
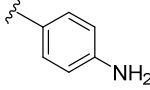
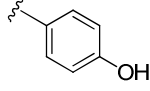
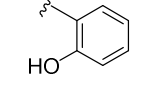
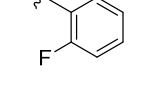
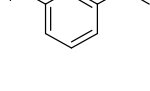
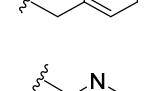
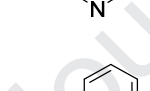
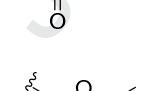
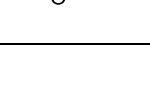
SAR study

Upon stimulation with CXCL8, the plasma membrane CXCR2 is phosphorylated and β -arrestins are recruited to their C terminus to cause the internalization of CXCR2, which mediates the activation of downstream signaling pathways including ERK1/2, JNK1, and p38 MAPK.³⁵⁻³⁷ Homologous CXCR4 trans-membrane protein triggers similar cascades as stimulated by stromal cell-derived factor 1 (SDF-1).³⁸ Tango assays based on beta-lactamase reporter provide a highly selective readout of target receptor activation and subsequent β -arrestin recruitment.³⁹ We tested all our compounds in both CXCR2 and CXCR4 Tango assays. A good selectivity for CXCR2 inhibition over CXCR4 was desirable as it indicates a more specific mechanism of action towards CXCR2, and could efficiently exclude experimental artifacts arising from the interferences with the assay.

Using a scaffold-hopping strategy, we first obtained compound **11**. Compound **11** inhibited CXCL8-mediated β -arrestin recruitment with an IC_{50} of $6.4 \pm 2.5 \mu M$ in CXCR2 Tango assay (Table 1). Encouraged by this result, we set out to investigate the SAR through the modification of the phenylthiourea moiety (Table 1). Most of the compounds were active in CXCR2 Tango assay and showed selectivity over CXCR4. Hydrophobic substituents at either para- meta- or ortho- positions were well tolerable (**12-19**, **23** and **24**), and compound **17** with a 2,2-difluorobenzo[d][1,3]dioxole moiety showed the best potency with an IC_{50} of $1.9 \pm 0.5 \mu M$. Hydrophilic groups like hydroxyl and amino groups (**20-22**) showed detrimental effect on their potencies, indicating phenylthiourea moiety is probably positioned in a hydrophobic cavity within its binding pocket. Replacement of the phenyl group with a benzyl (**25**) or an ethoxycarbonyl group (**28**) led to a slight decrease in potency while a pyrazine (**26**) or a benzoyl (**27**) group was not tolerated at this position.

Table 1. CXCR2/4 inhibition of TUTPs with modifications on the thiourea moiety

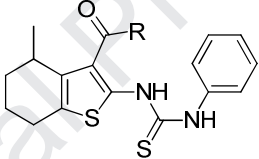
Compound	R	CXCR2 ^a	CXCR4 ^a	Selectivity of CXCR2/CXCR4	cLogP ^b
		IC ₅₀ (μM)	IC ₅₀ (μM)		
11		6.4±2.5	> 10	>1.6	5.05
12		2.1±0.7	11.7±1.3	5.5	5.25
13		4.4±2.0	11.5±6.5	2.6	5.00
14		2.2±1.3	12.7±5.5	5.7	6.10
15		3.9±0.7	> 10	>2.6	5.22
16		7.0±4.6	> 10	>1.4	6.88
17		1.9±0.5	26.7	14	6.52
18		7.7±0.6	>10	>1.3	4.62

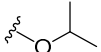
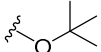
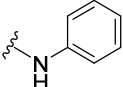
19		2.0±0.3	14.6±5.1	7.2	6.07
20		> 30	> 10	NA	3.83
21		> 30	11.7±2.7	<0.4	4.39
22		> 30	> 10	NA	4.39
23		7.5±2.3	12.0±2.8	>1.6	4.80
24		3.0±1.0	8.9±1.9	2.9	5.00
25		6.7 ±2.5	> 20	>3	5.53
26		> 10	> 10	NA	3.36
27		> 10	>10	NA	5.44
28		8.7±1.3	>10	>1.1	5.18

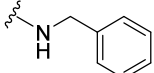
^aCXCR2/4 inhibition was determined by Tango assay and IC₅₀ values are the mean±SD of at least three independent experiments. ^bcLog P values were calculated using ChemBioDraw Professional 16.

We then investigated the effect of bioisosteric replacements of the ethyl ester moiety at position 3 of the tetrahydrobenzo[*b*]thiophene core (Table 2). The corresponding carboxylic acid showed a similar profile with the ethyl ester (**29**), while bulkier esters like isopropyl (**30**) or *tert*-butyl ester groups (**31**) were beneficial to the CXCR2 inhibition activity. A similar trend was observed within the amide analogs. Primary amide (**32**) or methyl amide (**33**) were not favored, which led to a complete loss of potency, whereas the phenyl (**34**) or benzyl (**35**) amides were active. Taken together, it is proposed that the carboxyl moiety is inserted into a hydrophobic cavity that requires a substantial volume.

Table 2. CXCR2/4 inhibition of TUTPs with modifications on the carboxyl moiety



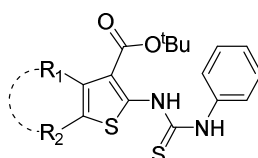
Compound	R	CXCR2	CXCR4	Selectivity of CXCR2/CXCR4	cLogP ^b
		IC ₅₀ ^a (μM)	IC ₅₀ ^a (μM)		
29		6.7±2.2	> 10	>1.5	4.79
30		2.7±1.2	9.3±1.1	3.4	5.36
31		2.5±1.4	11.9±0.4	4.9	5.76
32		>30	>10	NA	3.61
33		> 10	>10	NA	3.84
34		2.7±1.4	>10	>3.7	5.62

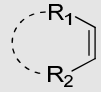
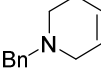
35		2.5±0.5	>30	>11.8	5.80
----	---	---------	-----	-------	------

^aCXCR2/4 inhibition was determined by Tango assay and IC₅₀ values are the mean ± SD of at least three independent experiments. ^bcLog P values were calculated using ChemBioDraw Professional 16.

The preliminary SAR study suggested that hydrophobic groups were generally favored on either the phenyl thiourea or the carboxyl moieties, such as compounds **30**, **31**, **34**, and **35**. However, these modification leads to cLogP value > 5, that can likely compromise aqueous solubility and simultaneously increases the risk of non-specific toxicity.³⁰ In view of this hypothesis, we proposed that the introduction of a hetero-atom into the hexane ring could possibly serve as a “lever” to balance the increase in cLogP by other hydrophobic moieties and thus be beneficial to overall physicochemical properties. As expected, dihydrothienopyran analogs **37** and **38** turned out to have desirable cLogP values and retained similar CXCR2 inhibition as compared to compound **31**. Moving the oxygen to other positions seemed not favorable as exemplified by compounds **39** and **40**. Replacement of the hexane with piperidines (**41-43**) diminished the activity of this series of compounds.

Table 3. CXCR2/4 inhibition of TUTPs with modifications on the tetrahydrobenzothiophene core



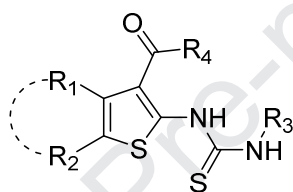
Compound		CXCR2	CXCR4	Selectivity of	cLogP ^b
		IC ₅₀ (μM)	IC ₅₀ (μM)	CXCR2/CXCR4	
36		1.8 ±0.3	>10	>5.6	5.24
37		1.7±1.3	>15	>8.8	3.66
38		2.3±2.0	>30	>13.2	3.14
39		4.1±1.7	>10	>2.4	4.25
40		>10	>10	NA	4.18
41		8.7±2.6	>10	>1.1	3.12
42		>10	>10	NA	3.57
43		> 10	>10	NA	5.56

^aCXCR2/4 inhibition was determined by Tango assay and IC₅₀ values are the mean±SD of at least three independent experiments. ^bcLog P values were calculated using ChemBioDraw Professional 16.

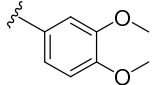
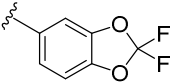
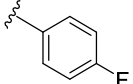
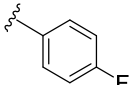
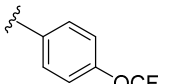
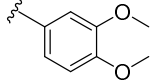
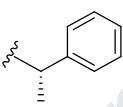
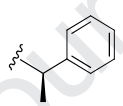
After exploring the favorable modifications on the core and substitutions individually, we then sought to investigate if the combination could be more beneficial to their potency and selectivity. Surprisingly, the *tert*-butyl ester group seemed not to be compatible with bulky substituents on the phenyl group when a tetrahydrobenzothiophene core was retained (**45-50**). Only compound **44** with a 3-methoxygroup showed a moderate potency. This incompatibility was also observed

when a dihydrothienopyran core structure was incorporated along with a phenyl amide moiety (**51**), which led to a complete loss of its activity. Gratifyingly, the dihydrothienopyran core was compatible with the *tert*-butyl ester group (**52-56**) where all compounds exhibited moderate to good potencies while retaining a good selectivity over CXCR4. Compound **52** was identified as the most potent CXCR2 antagonist ($IC_{50} = 1.1\mu M$) and it exhibited a 27-folds selectivity over CXCR4.

Table 4. CXCR2/4 inhibition of TUTPs with modifications on multiple sites



Compound		R ₃	R ₄	CXCR ₂ IC ₅₀ (μM)	CXCR ₄ IC ₅₀ (μM)	Selectivity of CXCR ₂ /CXCR ₄	cLogP ^b
44			O ^t Bu	2.7±2.1	>10	>3.7	5.70
45			O ^t Bu	10.6±3.6	>10	>0.9	6.81
46			O ^t Bu	6.8±2.5	>10	>1.5	6.94
47			O ^t Bu	>10	>10	NA	7.86
48			O ^t Bu	>10	>10	NA	5.66

49			O ^t Bu	5.7±2.0	>10	>1.8	5.33
50			O ^t Bu	>10	>10	NA	7.22
51			NHPh	>10	>10	NA	3.21
52			O ^t Bu	1.1±0.01	>30	>26.7	3.34
53			O ^t Bu	1.6±0.6	>30	>18.4	4.19
54			O ^t Bu	3.4±0.2	>10	>2.9	2.71
55			O ^t Bu	2.4±1.2	>30	>12.7	3.93
56			O ^t Bu	1.6±0.3	>30	>18.7	3.93
SB265610	-	-	-	0.15±0.02			-

^aCXCR2/4 inhibition was determined by Tango assay and IC₅₀ values are the mean±SD of at least three independent experiments. ^bcLog P values were calculated using ChemBioDraw Professional 16.

Different from the lead compound CX797 but similar to reported CXCR2 antagonist SB265610,⁴⁰ compound **52** selectively inhibited CXCL8-mediated β-arrestin recruitment (IC₅₀ = 1.1±0.01 μM, Figure 3). Compound **52** inhibited CXCL8-mediated recruitment of β-arrestin by ~87% at 10 μM, while CX797 cause an increase of ~117% of this signaling at the same

concentration. Both compounds had negligible effects on β -arrestin recruitment upon ligand stimulation with SDF-1. (Figure 3B). This result indicates that TUTPs represent a novel class of CXCR2 modulators with different mechanism of action on CXCR2 as compared with CX797.

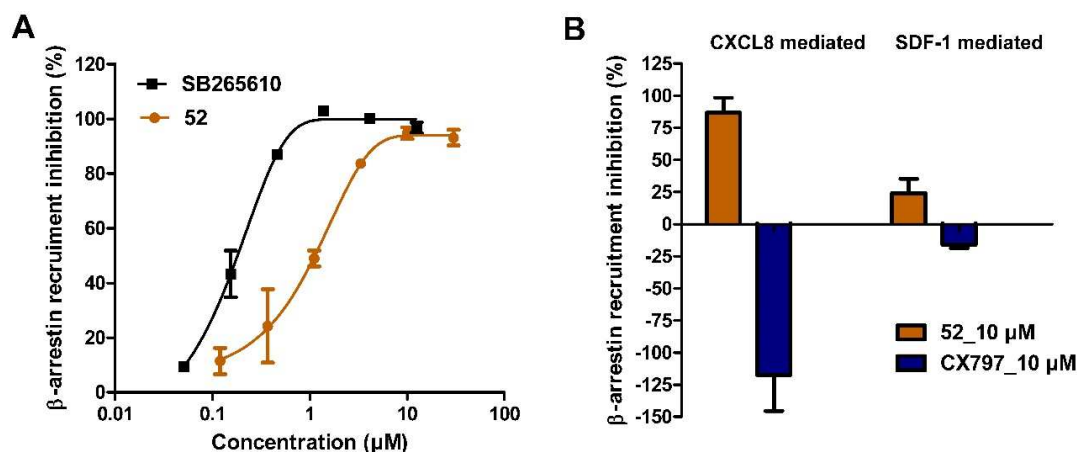


Figure 3. Compound **52** inhibited CXCL8-mediated β -arrestin recruitment, similar to the known CXCR2 antagonist SB265610 while different from CX797. (A) Dose-response curves of compound **52** and SB265610 in the CXCR2 TangoTM assay. (B) CX797 increased CXCL8-mediated β -arrestin recruitment while compound **52** inhibited CXCL8-mediated β -arrestin recruitment at the concentration of 10 μ M. Both compounds had negligible effects on β -arrestin recruitment upon ligand stimulation with SDF-1. CXCR2-bla U2OS cells were pre-treated with indicated concentrations of compounds for 30 min. Cells were then stimulated with CXCL8 for 5 h. Cells were loaded with a β -lactamase substrate for 2 h and the amount of cleaved and uncleaved substrate was measured using the Clario Star plate reader (excitation at 405 nm and emissions at 460 and 535 nm).

Compounds 37, 52 and 56 are selective over other GPCRs.

Compounds **37**, **52** and **56** were tested in a GPCR screening assay containing 50 different GPCRs (Supplementary Table S1 & S2). Compound **37** showed good selectivity over all the tested GPCRs (<50% inhibition at 10 μ M or K_i > 10 μ M in secondary binding assay) except binding to peripheral benzodiazepine receptor (PBR) at a K_i of 3.6 μ M (Table 5). Compounds **52** and **56** exhibited excellent selectivity over all the GPCRs tested, warranting their further development.

Table 5. GPCR inhibition screening results of compounds **37**, **52** and **56**

Compound	CXCR2	CXCR4	GPCRs with over 50% inhibition
	IC ₅₀ (μ M)	IC ₅₀ (μ M)	(K_i in secondary conformational binding assay) ^a
37	1.7 \pm 1.3	>15	PBR 63.1% (4.0 \pm 0.9 μ M)
			5-HT _{2B} 58.0% (>10 μ M)
			Alpha2A 55.2% (>10 μ M)
52	1.1 \pm 0.01	>30	None
56	1.6 \pm 0.3	>30	PBR 64.01% (>10 μ M)
			Alpha2A 59.01% (>10 μ M)

^a Compounds were screened in primary radioligand binding assays at a single concentration (10 μ M).

Compounds showing a minimum of 50% inhibition at 10 μ M are tagged for secondary radioligand binding assays to determine equilibrium binding affinity at specific targets.

TUTP Compounds Do Not Interfere with CXCL8-mediated cAMP signaling and calcium mobilization

Besides β -arrestin recruitment, G-protein signaling is another main cascade involved in CXCL8-CXCR2 axis. G-protein activation inhibits adenylyl cyclase resulting in decreased cAMP production and induces rapid intracellular Ca^{2+} mobilization released from the endoplasmic reticulum (ER). We measured the level of those second messengers (cAMP and calcium) upon **52** and **56** treatment.

293T-CXCR2-GFP-p22F cells was engineered to express the cAMP sensitive firefly luciferase which served as readout of the cAMP level.⁴¹ Forskolin activates the enzyme adenylyl cyclase and increases intracellular levels of cAMP as shown in Figure 4A, while the addition of CXCL8 inhibit the stimulation of cAMP signaling. The treatment of SB265610 and CX797 blocked the inhibition of cAMP production caused by CXCL8 treatment, while TUTP compound **52** and **56** did not.

As shown in Figure 4B, CXCL8 rapidly induces calcium mobilization in 293T-CXCR2-GFP cells, reaching a peak within 30 s. Pre-treatment with 15 μM SB265610 significantly reduced CXCL8-mediated calcium mobilization. However, co-treatment with TUTP compound **52** or CX797 had negligible effect on calcium flux. This observation demonstrates that although TUTP compounds inhibit CXCL8-mediated β -arrestin recruitment, they don't show significant effect on cAMP signaling and calcium mobilization, suggesting that TUTP compounds have a biased impact on CXCR2 downstream signaling.

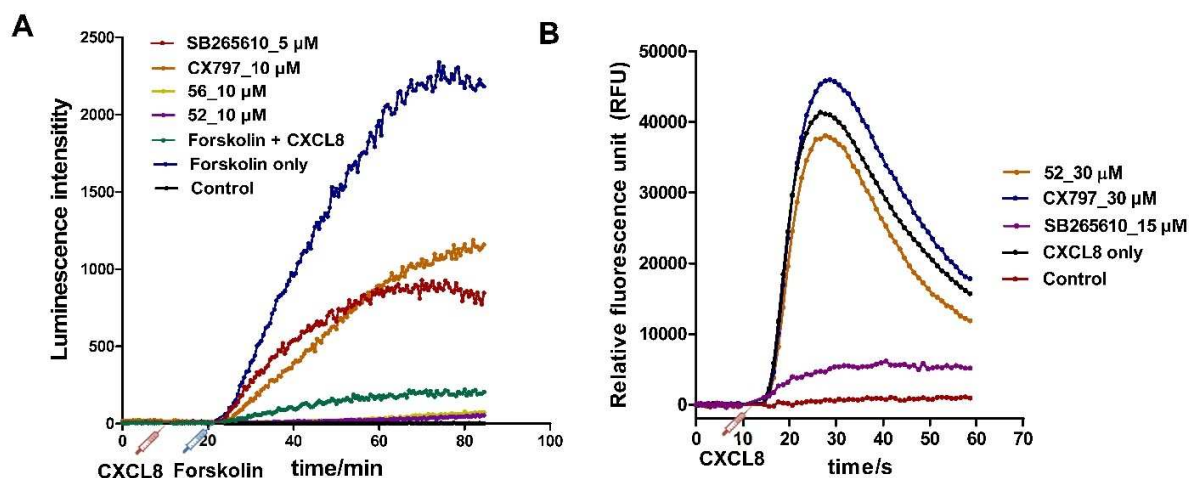


Figure 4. TUTP compounds did not inhibit CXCL8-mediated cAMP signaling and calcium mobilization. (A) CX797 and SB265610 inhibited CXCL8-mediated, forskolin-stimulated cAMP signaling while TUTP compounds **52** and **56** did not. Cells were pretreated with compounds at indicated concentrations for 10 min prior to stimulation with 50 nM of CXCL8. Cells were then stimulated with 50 μ M of forskolin until max signal was reached (~80 min). (B) **52** and CX797 did not inhibit CXCL8 induced calcium mobilization in CXCR2-overexpressing 293T-CXCR2-GFP cells. The cells were pretreated with compounds before the addition of CXCL8 (300 nM) through injector. SB265610 inhibited CXCL8-stimulated calcium internalization while **52** and CX797 did not.

TUTP Compounds Inhibit CXCL8-CXCR2 mediated ERK1/2 Phosphorylation

After the stimulation of CXCR2 by CXCL8, both β -arrestin recruitment and G-protein-mediated signaling result in phosphorylation of ERK1/2, which promotes chemotaxis. Other growth and stress proteins such as P38, JNK, cJUN, and AKT are also stimulated to facilitate cell survival and proliferation.^{2, 35-37} The impact of TUTP compounds on ERK1/2 phosphorylation and other downstream signaling was investigated. We observed that CXCL8 treatment induced

phosphorylation of ERK1/2 in T293-CXCR2-GFP cells in a dose-dependent manner (Figure 5A). Using 60 nM of CXCL8 to stimulate phosphorylation of ERK1/2, pretreatment with SB265610 (10 μ M) or TUTP compound **52** and **56** blocked CXCL8-induced ERK1/2 phosphorylation (Figure 5B). In contrast, CX797 stimulated ERK1/2 phosphorylation. The increased phosphorylation of P38, JNK, cJUN, and AKT was also observed post-CXCL8 treatment that could not be reversed by SB265610 or TUTP compounds treatment (Figure 5C).

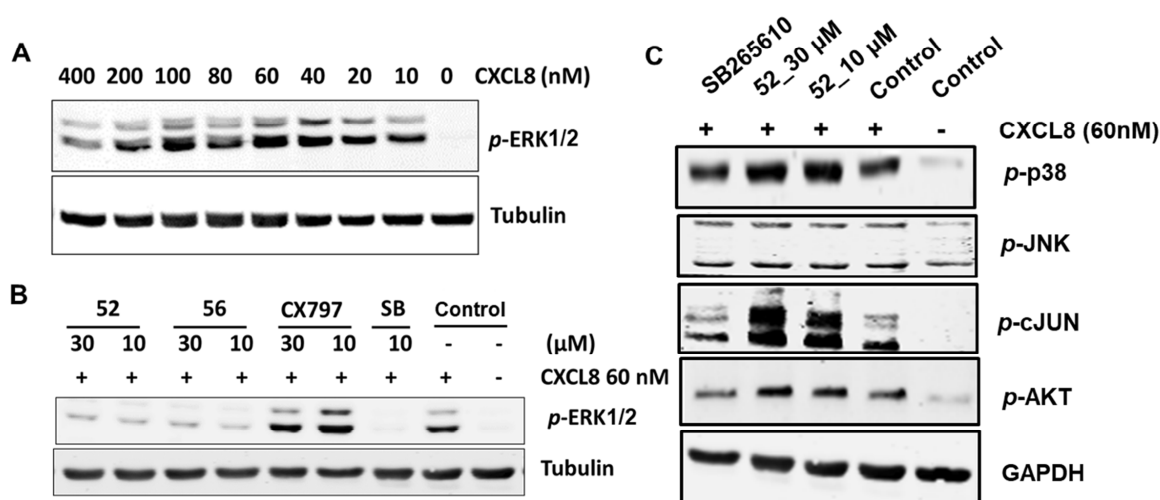


Figure 5. The influences of TUTPs on the CXCL8-CXCR2 down-stream cell signaling pathway. (A) Dose-response of CXCL8 stimulated phosphorylation of ERK1/2. 60 nM of CXCL8 is used in the subsequent experiments. (B) SB265610 (SB), TUTP compounds **52** and **56** inhibited the phosphorylation of ERK1/2 while CX797 enhanced the phosphorylation of ERK1/2. (C) 60 nM CXCL8 treatment lead to the enhanced phosphorylation of P38, JNK, cJUN, and AKT, which were not inhibited by SB265610 or TUTP compound **52**.

TUTP compound inhibited the cell migration in the wound healing assay

CXCL8-CXCR2 mediates the chemotaxis of neutrophils and endothelial cells during infection and angiogenesis.⁴² CXCL8 also induce cancer cell migration and invasion.⁴³ Thus, we used a wound healing assay to assess the effects of selected TUTP compounds on CXCL8-induced cell migration (Figure 6). Treatment of U2OS cells with CXCL8 induced cell migration and promoted wound healing as compared to the unstimulated control group. Pretreatment with **52**, **56** or SB265610 prior to CXCL8 stimulation inhibited CXCL8-mediated wound closure.

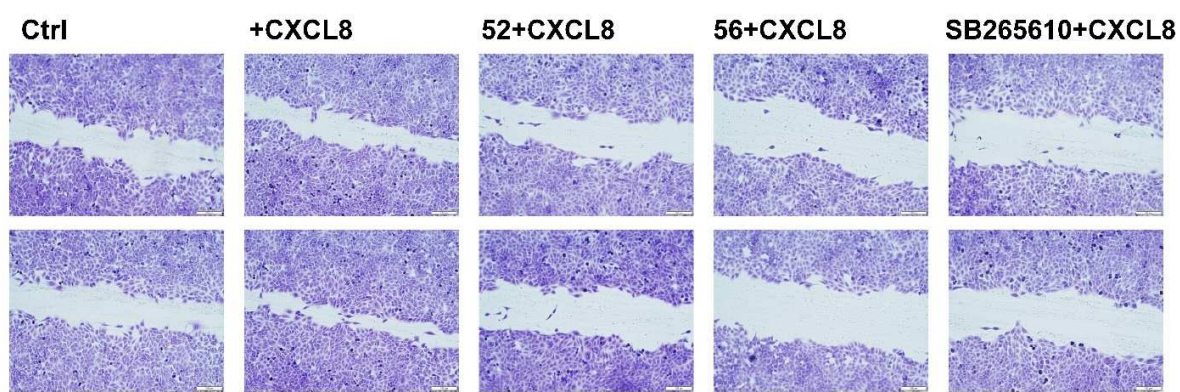


Figure 6. TUTP compounds and SB265610 inhibited CXCL8-mediated cell migration. (A) CXCR2-bla U2OS were seeded in 96-well plates at 35, 000 cells per well in DMEM supplemented with 1% FBS overnight. A single wound was induced in the monolayer with a sterile pipette tip and washed with PBS. Cells were treated with TUTP compounds (10 μ M) or SB265610 (10 μ M) for 20 min and then stimulated with CXCL8 (60 nM) for 24 h. Control wells were not stimulated with CXCL8. +CXCL8 wells were treated with CXCL8 (60 nM). Representative images of two independent experiments performed in duplicate are shown here.

Combination of TUTP Compounds and Doxorubicin is Synergistic in Ovarian Cancer Cells

Inflammatory chemokines play an important role in the angiogenesis and progression of ovarian cancer. The interactions between chemokines produced by the ovarian cancer cells and chemokine receptors expressed by endothelial cells and the tumor microenvironment promote tumor growth by stimulating angiogenesis and increasing migration, invasion, and cell proliferation.^{44, 45} CXCR2 inhibition combined with sorafenib improved antitumor and antiangiogenic response in preclinical models of ovarian cancer.⁴⁶ We investigated the combination of selected TUTP compounds with several anticancer drugs in ovarian cancer cell lines. Results showed that compound **52**, **56** or **37** was synergistic with doxorubicin in SKOV3 cells (Figure 7). Doxorubicin did not show significant cytotoxicity in SKOV3 cells at the concentration up to 38 nM. However, combination with TUTP compounds (8.9 μ M, 13.3 μ M and 20 μ M) resulted in significant inhibition of colony formation. Compound **56** exerted the best synergistic effect in the colony formation assay. This result indicates that TUTP compounds hold the potential to aid standard-of-care cancer chemotherapies.

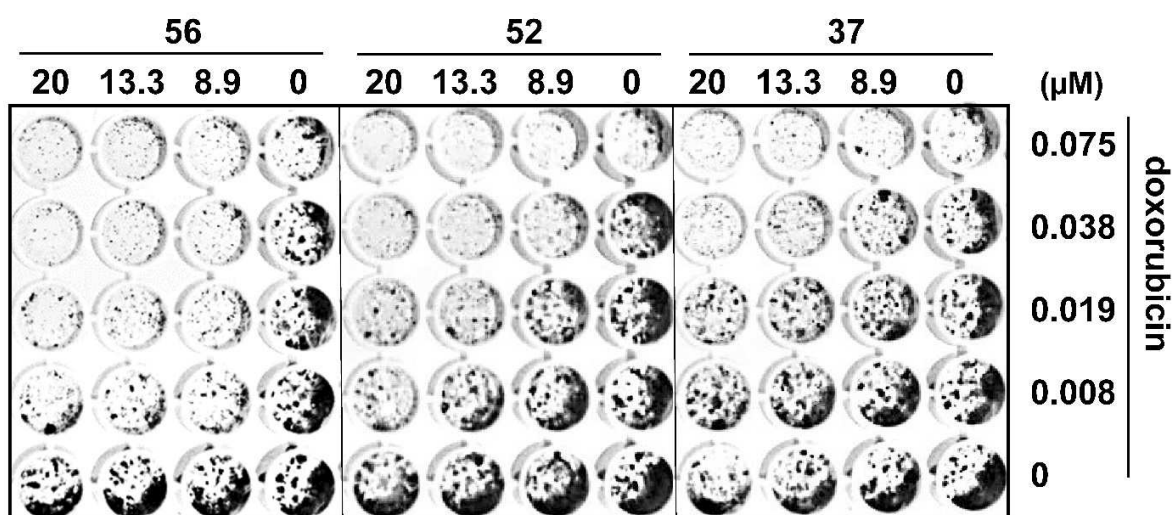


Figure 7. The combination of TUTP compounds (**56**, **52** or **37**) with doxorubicin exerted synergistic anticancer activity against SKOV3 cells in colony formation assay.

CONCLUSION

Our previous study has identified a pyrimidine-based compound CX797 as a modulator of CXCR2/CXCL8 signaling, which inhibited CXCL8-mediated cAMP signaling while specifically up-regulated CXCL8-mediated β -arrestin recruitment (Figure 8). In this study, structure modification of CX797 by a scaffold-hopping approach resulted in the discovery of a series of TUTP compound as novel CXCR2 antagonists. An extensive SAR study was carried out and the most potent compound **52** obtained inhibited β -arrestin recruitment with an IC_{50} of 1.1 μ M in Tango assay. In addition, select TUTP compounds showed good selectivity for CXCR2 inhibition over CXCR4 and other GPCRs, further implicating they are specific CXCR2 antagonists.

Interestingly, TUTP compound **52** inhibited CXCL8/CXCR2 β -arrestin coupling cascade while does not interfere with the G-protein signaling mediated by second messengers cAMP or calcium. Similar to CXCR2 antagonist SB265610, TUTP **52** also inhibited phosphorylation of ERK1/2 induced by CXCR2 activation (Figure 8). Because of the complexity and flexibility of the transmembrane protein, multiple antagonist allosteric binding sites are reported to exist in the transmembrane regions and C-terminal domains.⁴⁷ Meanwhile, different regions of CXCR2 such as C/N-terminus, transmembrane domain and loop specifically contribute to ligand binding and specificity, receptor desensitization and endocytosis, receptor phosphorylation, and G-protein coupling.² Therefore, antagonists with different binding sites on CXCR2 could behave differently in modulating the down-stream signaling of CXCR2/CXCL8 axis. It is most likely

that TUTP compounds act as biased ligands and their interaction with CXCR2 does not shut down the entire receptor. Some other biased ligands that selectively alter GPCR-mediated signaling have been reported in GPCRs including CXCR2, CXCR4 and CXCR7.^{36, 48-51}

We also demonstrated that TUTP compounds inhibited cancer cell migration induced by CXCL8, which is an important driver of tumor metastasis. TUTP compounds also exhibited synergistic effect with doxorubicin in ovarian cancer cells at non cytotoxic concentrations, which may be advantageous for aiding standard-of-care chemotherapies. Additionally, further development and characterization of TUTP compounds will offer important insights into CXCR2 signaling and function, facilitating the design and application of CXCR2 inhibitors.

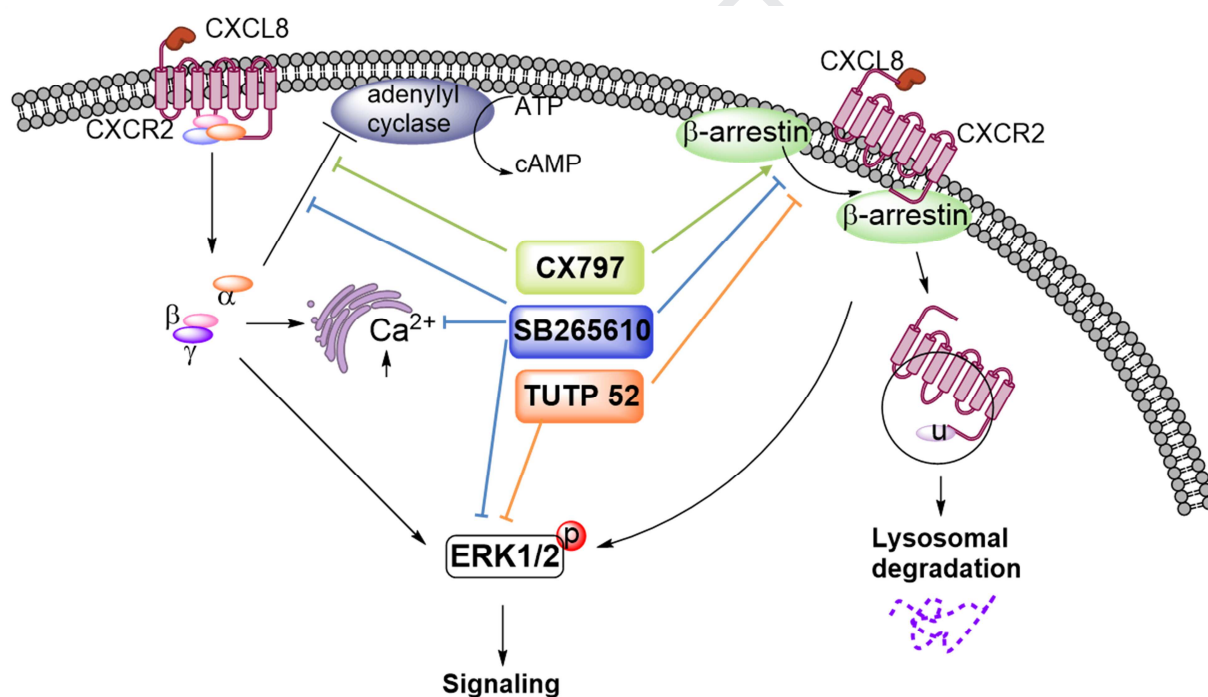


Figure 8. Schematic illustration of the proposed mechanism of action of CX797, TUTP compound **52** and SB265610.

EXPERIMENTAL SECTION

Chemistry. Unless otherwise specified, all reactions were carried out in oven-dried glassware with magnetic stirring. All commercial reagents and anhydrous solvents were purchased and used without purification, unless specified. Column chromatography was performed on silica gel (200–300 mesh). Preparative HPLC was performed on Shimadzu LC20-AT system, using Kinetex® 5 μm , XB-C18 100 \AA , 150 x 21.2 mm column at room temperature. HPLC gradient method utilized was 10% to 95% MeCN in H₂O with 0.05% trifluoroacetic acid over 25 minutes with a 8 mL/min flow rate. NMR spectra were recorded on a Bruker 300 or 400MHz NMR spectrometer. Chemical shifts for proton magnetic resonance spectra (¹H NMR) and carbon magnetic resonance spectra (¹³C NMR) are quoted in parts per million (ppm) referenced to the appropriate solvent peak or 0.0 ppm for tetramethylsilane (TMS). The following abbreviations are used to describe the peak-splitting patterns when appropriate: br, broad; s, singlet; d, doublet; t, triplet; q, quartet; m, multiplet; and dd, doublet of doublets. Coupling constants, J, are reported in hertz (Hz). All compounds were $\geq 95\%$ purity as determined by Shimadzu LC-2030C 3D liquid chromatography system using Kinetex® 2.6 μm , XB-C18 100 \AA , 75 x 4.6 mm column at room temperature. HPLC gradient method utilized was 10% to 95% MeCN in H₂O with 0.1% formic acid over 15 minutes with a 0.80 mL/min flow rate. Mass spectra were recorded using ESI ion source on a Shimadzu LCMS-2020 system.

Ethyl 2-amino-4-methyl-4,5,6,7-tetrahydrobenzo[b]thiophene-3-carboxylate (2a). A mixture of 2-methylcyclohexanone (33.6 g, 0.3 mol), ethyl 2-cyanoacetate (33.9 g, 0.3 mol), sulfur (9.6 g, 0.3 mol) and morpholine (26.1 g, 0.3 mol) were stirred at room temperature for 48 h. The mixture was directly purified with silica chromatography (5% EtOAc in hexane) to give a pale yellow solid (30.1 g, 42%). ¹H NMR (400 MHz, CDCl₃) δ 4.37–4.19 (m, 2H), 3.30–3.19 (m,

1H), 2.52–2.45 (m, 2H), 1.94–1.70 (m, 3H), 1.67–1.58 (m, 1H), 1.35 (t, $J = 7.1$ Hz, 3H), 1.15 (d, $J = 6.8$ Hz, 3H). LC-MS (ESI) m/z 240.1 [M + H]⁺.

Isopropyl 2-amino-4-methyl-4,5,6,7-tetrahydrobenzo[b]thiophene-3-carboxylate (2b). Using a similar procedure as described for **2a** with 2-methylcyclohexanone (560 mg, 5.0 mmol), isopropyl 2-cyanoacetate (635 mg, 5.0 mmol), sulfur (160 mg, 5.0 mmol) and morpholine (435 mg, 5.0 mmol) and purified with silica chromatography (20% EtOAc in hexane). Light yellow solid (806 mg, 64%). ¹H NMR (300 MHz, CDCl₃) δ 5.22 (p, $J = 6.2$ Hz, 1H), 3.30 (d, $J = 12.4$ Hz, 1H), 2.53 (s, 2H), 1.98–1.61 (m, 4H), 1.36 (t, $J = 6.6$ Hz, 6H), 1.18 (d, $J = 6.8$ Hz, 3H).

tert-Butyl 2-amino-4-methyl-4,5,6,7-tetrahydrobenzo[b]thiophene-3-carboxylate (2c). Using a similar procedure as described for **2a** with 2-methylcyclohexanone (794 mg, 7.1 mmol), tert-butyl 2-cyanoacetate (1.0 g, 7.1 mmol), sulfur (227 mg, 7.1 mmol) and morpholine (617 mg, 7.1 mmol), and purified with silica chromatography (10% EtOAc in hexane). White solid (1.38 g, 73%). ¹H NMR (300 MHz, CDCl₃) δ 3.25 (t, $J = 6.3$ Hz, 1H), 2.51 (s, 2H), 1.94–1.61 (m, 5H), 1.58 (s, 8H), 1.18 (d, $J = 6.8$ Hz, 3H).

2-Amino-4-methyl-4,5,6,7-tetrahydrobenzo[b]thiophene-3-carboxamide (2d). Using a similar procedure as described for **2a** with 2-methylcyclohexanone (667 mg, 6.0 mmol), 2-cyanoacetamide (500 mg, 6.0 mmol), sulfur (190 mg, 6.0 mmol) and morpholine (518 mg, 6.0 mmol), and purified with silica chromatography (10% MeOH in DCM). Light yellow solid (213 mg, 17%). ¹H NMR (300 MHz, CDCl₃) δ 3.08 (t, $J = 6.6$ Hz, 1H), 2.51 (t, $J = 5.9$ Hz, 2H), 1.97–1.56 (m, 4H), 1.17 (d, $J = 6.9$ Hz, 3H). LC-MS (ESI) m/z 211.1 [M + H]⁺.

tert-Butyl 2-amino-4,5,6,7-tetrahydrobenzo[b]thiophene-3-carboxylate (2e). Using a similar procedure as described for **2a** with cyclohexanone (500 mg, 5.1 mmol), tert-butyl 2-cyanoacetate (719 mg, 5.1 mmol), sulfur (163 mg, 5.1 mmol) and morpholine (444 mg, 5.1 mmol), and

purified with silica chromatography (10% EtOAc in hexane). White solid (1.0 g, 78%). ^1H NMR (300 MHz, CDCl_3) δ 2.72–2.65 (m, 2H), 2.55–2.48 (m, 2H), 1.82–1.73 (m, 4H), 1.56 (s, 9H).

tert-Butyl 2-amino-4-methyl-5,7-dihydro-4H-thieno[2,3-c]pyran-3-carboxylate (2f). Using a similar procedure as described for **2a** with 3-methyldihydro-2H-pyran-4(3H)-one (150 mg, 1.32 mmol), *tert*-butyl 2-cyanoacetate (186 mg, 1.32 mmol), sulfur (42 mg, 1.32 mmol) and morpholine (115 mg, 1.32 mmol), and purified with silica chromatography (20% EtOAc in hexane). Light yellow solid (286 mg, 81%). ^1H NMR (300 MHz, CDCl_3) δ 4.66–4.52 (m, 2H), 3.90–3.74 (m, 2H), 3.04 (d, $J = 7.4$ Hz, 1H), 1.58 (s, 9H), 1.31 (d, $J = 6.8$ Hz, 3H).

tert-Butyl 2-amino-5,7-dihydro-4H-thieno[2,3-c]pyran-3-carboxylate (2g). Using a similar procedure as described for **2a** with dihydro-2H-pyran-4(3H)-one (500 mg, 5.0 mmol), *tert*-butyl 2-cyanoacetate (705 mg, 5.0 mmol), sulfur (160 mg, 5.0 mmol) and morpholine (435 mg, 5.0 mmol) and purified with silica chromatography (20% EtOAc in hexane). White solid (1.18 g, 92%). ^1H NMR (300 MHz, CDCl_3) δ 4.56 (d, $J = 2.1$ Hz, 2H), 3.91 (t, $J = 5.6$ Hz, 2H), 2.85–2.75 (m, 2H), 1.55 (s, 9H).

tert-Butyl 6-amino-3,4-dihydro-2H-thieno[2,3-b]pyran-5-carboxylate (2h). Using a similar procedure as described for **2a** with dihydro-2H-pyran-3(4H)-one (300 mg, 3.0 mmol), *tert*-butyl 2-cyanoacetate (423 mg, 3.0 mmol), sulfur (96 mg, 3.0 mmol) and morpholine (261 mg, 3.0 mmol), and purified with silica chromatography (20% EtOAc in hexane). Light yellow solid (425 mg, 56%). ^1H NMR (300 MHz, CDCl_3) δ 4.20–4.11 (m, 2H), 2.68 (t, $J = 6.5$ Hz, 2H), 1.99 (dt, $J = 10.8, 6.2$ Hz, 2H), 1.55 (s, 9H).

tert-Butyl 2-amino-6,6-dimethyl-6,7-dihydro-4H-thieno[3,2-c]pyran-3-carboxylate (2i). Using a similar procedure as described for **2a** with 6,6-dimethyldihydro-2H-pyran-3(4H)-one (300 mg, 2.34 mmol), *tert*-butyl 2-cyanoacetate (330 mg, 2.34 mmol), sulfur (75 mg, 2.34 mmol) and

morpholine (204 mg, 2.34 mmol), and purified with silica chromatography (20% EtOAc in hexane). Light yellow solid (492 mg, 74%). $^1\text{H NMR}$ (300 MHz, CDCl_3) δ 4.57 (s, 2H), 2.67 (s, 2H), 1.57 (s, 9H), 1.31 (s, 6H).

*tert-Butyl 2-amino-6-methyl-4,5,6,7-tetrahydrothieno[2,3-*c*]pyridine-3-carboxylate (2j)*. Using a similar procedure as described for **2a** with 1-methylpiperidin-4-one (500 mg, 4.42 mmol), tert-butyl 2-cyanoacetate (624 mg, 4.42 mmol), sulfur (141 mg, 4.42 mmol) and morpholine (385 mg, 4.42 mmol), and purified with silica chromatography (10% MeOH in DCM). White solid (754 mg, 64%). $^1\text{H NMR}$ (300 MHz, CDCl_3) δ 5.94 (s, 2H), 3.38 (t, $J = 2.0$ Hz, 2H), 2.82 (ddt, $J = 5.6, 4.1, 2.0$ Hz, 2H), 2.67 (t, $J = 5.8$ Hz, 2H), 2.45 (s, 3H), 1.55 (s, 9H). LC-MS (ESI) m/z 269.0 [$\text{M} + \text{H}$] $^+$.

*tert-Butyl 2-amino-6-benzyl-4,5,6,7-tetrahydrothieno[2,3-*c*]pyridine-3-carboxylate (2k)*. Using a similar procedure as described for **2a** with 1-benzylpiperidin-4-one (500 mg, 2.65 mmol), tert-butyl 2-cyanoacetate (374 mg, 2.65 mmol), sulfur (85 mg, 2.65 mmol) and morpholine (231 mg, 2.65 mmol), and purified with silica chromatography (20% EtOAc in hexane). Light yellow solid (880 mg, 97%). $^1\text{H NMR}$ (300 MHz, CDCl_3) δ 7.52–7.30 (m, 5H), 5.94 (s, 2H), 3.72 (s, 2H), 3.45 (s, 2H), 2.92–2.67 (m, 4H), 1.54 (s, 9H).

*tert-Butyl 2-amino-4,5,6,7-tetrahydrothieno[2,3-*c*]pyridine-3-carboxylate (2l)*. Using a similar procedure as described for **2a** with piperidin-4-one (230 mg, 2.32 mmol), tert-butyl 2-cyanoacetate (327 mg, 2.32 mmol), sulfur (74 mg, 2.32 mmol) and morpholine (202 mg, 2.32 mmol), and purified with silica chromatography (10% MeOH in DCM with 1% NH_4OH). Yellow solid (228 mg, 39%). $^1\text{H NMR}$ (300 MHz, CDCl_3) δ 6.01 (s, 2H), 3.83 (s, 2H), 3.12 (t, $J = 5.9$ Hz, 2H), 2.88 – 2.70 (m, 4H), 1.55 (s, 9H). LC-MS (ESI) m/z 255.1 [$\text{M} + \text{H}$] $^+$.

Ethyl 4-methyl-2-(3-phenylthioureido)-4,5,6,7-tetrahydrobenzo[b]thiophene-3-carboxylate (11).

A mixture of **2a** (18.0 g, 0.075 mol) and phenyl isothiocyanate (10.6 g, 0.079 mol) were heated in pyridine (120 mL) at 60 °C for 5h. The solvent was removed by evaporation. MeOH was added to the residue and white solid was generated. The mixture was filtered, and the solid was washed by MeOH to give **11** as a white solid. (26.1 g, 93%). ¹H NMR (300 MHz, CDCl₃) δ 12.22 (s, 1H), 7.94 (s, 1H), 7.47 (t, *J* = 6.0 Hz, 2H), 7.40–7.31 (m, 3H), 4.22–4.06 (m, 2H), 3.29 (t, *J* = 6.7 Hz, 1H), 2.73–2.53 (m, 2H), 1.93–1.70 (m, 3H), 1.68–1.59 (m, 1H), 1.26 (t, *J* = 7.1 Hz, 3H), 1.11 (d, *J* = 6.8 Hz, 3H). LC-MS (ESI) *m/z* 375.1 [M + H]⁺. ¹³C NMR (101 MHz, CDCl₃) δ 176.24, 166.13, 150.36, 136.07, 135.88, 130.01, 127.76, 126.39, 125.74, 112.62, 60.45, 29.93, 28.94, 24.35, 21.88, 18.11, 14.03. Purity 98.4%.

Ethyl 4-methyl-2-(3-(pyrazin-2-yl)thioureido)-4,5,6,7-tetrahydrobenzo[b]thiophene-3-carboxylate (26). Using a similar procedure as described for **11** with **2a** (93 mg, 0.39 mmol) and 2-isothiocyanatopyrazine (64 mg, 0.47 mmol), white solid (75 mg, 51%). ¹H NMR (300 MHz, CDCl₃) δ 14.99 (s, 1H), 8.77 (s, 1H), 8.43 (dd, *J* = 2.7, 1.4 Hz, 1H), 8.39 (d, *J* = 1.5 Hz, 1H), 8.34 (d, *J* = 2.7 Hz, 1H), 4.52–4.31 (m, 2H), 3.42 (d, *J* = 6.8 Hz, 1H), 2.81–2.54 (m, 2H), 1.98–1.66 (m, 4H), 1.43 (t, *J* = 7.1 Hz, 3H), 1.19 (d, *J* = 6.8 Hz, 3H). LC-MS (ESI) *m/z* 377.0 [M + H]⁺. Purity 98.8%.

Ethyl 2-(3-benzoylthioureido)-4-methyl-4,5,6,7-tetrahydrobenzo[b]thiophene-3-carboxylate (27).

Using a similar procedure as described for **11** with **2a** (60 mg, 0.25 mmol) and benzoyl isothiocyanate (41 mg, 0.25 mmol), light yellow solid (75 mg, 75%). ¹H NMR (300 MHz, CDCl₃) δ 14.83 (s, 1H), 9.12 (s, 1H), 7.97 (dd, *J* = 7.2, 1.8 Hz, 2H), 7.71–7.61 (m, 1H), 7.55 (dd, *J* = 8.4, 6.9 Hz, 2H), 4.63–4.41 (m, 2H), 3.46 (d, *J* = 6.7 Hz, 1H), 2.83–2.57 (m, 2H), 2.01–1.68 (m, 4H),

1.44 (t, $J = 7.1$ Hz, 3H), 1.21 (d, $J = 6.8$ Hz, 3H). LC-MS (ESI) m/z 403.0 $[M + H]^+$. Purity 99.1%.

Ethyl 2-(3-(ethoxycarbonyl)thioureido)-4-methyl-4,5,6,7-tetrahydrobenzo[b]thiophene-3-carboxylate (28). Using a similar procedure as described for **11** with **2a** (50 mg, 0.21 mmol) and O-ethyl carbonisothiocyanatide (28 mg, 0.21 mmol), white solid (61 mg, 79%). $^1\text{H NMR}$ (300 MHz, CDCl_3) δ 14.10 (s, 1H), 8.10 (s, 1H), 4.57–4.30 (m, 4H), 3.43 (d, $J = 6.6$ Hz, 1H), 2.80–2.53 (m, 2H), 1.98–1.68 (m, 4H), 1.38 (dt, $J = 18.2, 7.1$ Hz, 6H), 1.18 (d, $J = 6.8$ Hz, 3H). LC-MS (ESI) m/z 369.2 $[M - H]^-$. Purity 99.0%.

Isopropyl 4-methyl-2-(3-phenylthioureido)-4,5,6,7-tetrahydrobenzo[b]thiophene-3-carboxylate (30). Using a similar procedure as described for **11** with **2b** (80 mg, 0.32 mmol) and phenyl isothiocyanate (43 mg, 0.32 mmol), white solid (80 mg, 65%). $^1\text{H NMR}$ (300 MHz, CDCl_3) δ 12.40 (s, 1H), 7.85 (s, 1H), 7.49 (t, $J = 7.6$ Hz, 2H), 7.37 (dd, $J = 11.6, 7.3$ Hz, 3H), 5.05 (p, $J = 6.2$ Hz, 1H), 3.31 (s, 1H), 2.76–2.57 (m, 2H), 1.80 (d, $J = 14.7$ Hz, 4H), 1.27 (dd, $J = 9.0, 6.3$ Hz, 6H), 1.13 (d, $J = 6.8$ Hz, 3H). LC-MS (ESI) m/z 389.1 $[M + H]^+$. Purity 98.4%.

tert-Butyl 4-methyl-2-(3-phenylthioureido)-4,5,6,7-tetrahydrobenzo[b]thiophene-3-carboxylate (31). Using a similar procedure as described for **11** with **2c** (500 mg, 1.87 mmol) and phenyl isothiocyanate (253 mg, 1.87 mmol), white solid (444 mg, 59%). $^1\text{H NMR}$ (300 MHz, CDCl_3) δ 12.49 (s, 1H), 7.82 (s, 1H), 7.47 (dd, $J = 8.3, 6.7$ Hz, 2H), 7.43–7.31 (m, 3H), 3.26 (d, $J = 7.0$ Hz, 1H), 2.76–2.49 (m, 2H), 1.92–1.58 (m, 4H), 1.46 (s, 9H), 1.13 (d, $J = 6.8$ Hz, 3H). LC-MS (ESI) m/z 403.1 $[M + H]^+$. Purity 99.3%.

4-Methyl-2-(3-phenylthioureido)-4,5,6,7-tetrahydrobenzo[b]thiophene-3-carboxylic acid (29).

To a solution of **31** (444 mg, 1.10 mmol) in DCM (3 mL) was added TFA (0.75 mL) dropwise and stirred at room temperature for 2 h. The mixture was concentrated, diluted by EtOAc and

extracted by 0.5N NaOH (20 mL) for three times. The aqueous layer was adjusted to pH 3 by concentrated HCl then 1N HCl and filtered to give a white solid. (149 mg, 39%). ^1H NMR (300 MHz, CDCl_3) δ 7.42 (d, $J = 6.6$ Hz, 4H), 7.33–7.24 (m, 1H), 3.37 (d, $J = 5.7$ Hz, 1H), 2.74–2.52 (m, 2H), 2.00–1.61 (m, 4H), 1.18 (d, $J = 6.8$ Hz, 3H). LC-MS (ESI) m/z 347.0 $[\text{M} + \text{H}]^+$. Purity 99.1%.

4-Methyl-2-(3-phenylthioureido)-4,5,6,7-tetrahydrobenzo[b]thiophene-3-carboxamide (32).

Using a similar procedure as described for **11** with **2d** (42 mg, 0.20 mmol) and phenyl isothiocyanate (24 mg, 0.20 mmol), and then purified with prep-HPLC to give a white solid (15 mg, 22%). ^1H NMR (300 MHz, CDCl_3) δ 12.79 (s, 1H), 7.90 (s, 1H), 7.50 (t, $J = 7.6$ Hz, 2H), 7.37 (dd, $J = 16.0, 7.5$ Hz, 3H), 5.86 (s, 2H), 2.94 (d, $J = 7.9$ Hz, 1H), 2.67 (qd, $J = 8.9, 15.8$ Hz, 2H), 1.80 (td, $J = 10.4, 25.4, 27.9$ Hz, 6H), 1.24 (d, $J = 6.9$ Hz, 3H). LC-MS (ESI) m/z 346.0 $[\text{M} + \text{H}]^+$. Purity 98.5%.

tert-Butyl 2-(3-phenylthioureido)-4,5,6,7-tetrahydrobenzo[b]thiophene-3-carboxylate (36).

Using a similar procedure as described for **11** with **2e** (77 mg, 0.24 mmol) and phenyl isothiocyanate (33 mg, 0.24 mmol), white solid (66 mg, 71%). ^1H NMR (300 MHz, CDCl_3) δ 12.41 (s, 1H), 7.83 (s, 1H), 7.47 (dd, $J = 8.3, 6.7$ Hz, 2H), 7.42–7.31 (m, 3H), 2.67 (dt, $J = 12.9, 5.6$ Hz, 4H), 1.86–1.71 (m, 4H), 1.45 (s, 9H). LC-MS (ESI) m/z 389.1 $[\text{M} + \text{H}]^+$. Purity 100.0%.

tert-Butyl 4-methyl-2-(3-phenylthioureido)-5,7-dihydro-4H-thieno[2,3-c]pyran-3-carboxylate

(37). Using a similar procedure as described for **11** with **2f** (50 mg, 0.19 mmol) and phenyl isothiocyanate (25 mg, 0.19 mmol), white solid (48 mg, 63%). ^1H NMR (300 MHz, CDCl_3) δ 12.46 (s, 1H), 7.49 (t, $J = 7.5$ Hz, 2H), 7.38 (dd, $J = 13.9, 7.2$ Hz, 3H), 4.71 (q, $J = 14.6$ Hz, 2H), 3.89–3.75 (m, 2H), 3.05 (d, $J = 6.9$ Hz, 1H), 1.47 (s, 9H), 1.27 (d, $J = 6.8$ Hz, 3H). LC-MS (ESI)

m/z 405.1 $[M + H]^+$. ^{13}C NMR (101 MHz, $CDCl_3$) δ 176.42, 165.66, 151.04, 135.80, 133.92, 129.94, 127.81, 126.03, 123.28, 113.18, 82.24, 70.86, 64.77, 30.95, 28.10, 20.17. Purity 95.2%.

tert-Butyl 2-(3-phenylthioureido)-5,7-dihydro-4H-thieno[2,3-c]pyran-3-carboxylate (38). Using a similar procedure as described for **11** with **2g** (50 mg, 0.20 mmol) and phenyl isothiocyanate (26 mg, 0.20 mmol), white solid (64 mg, 82%). 1H NMR (300 MHz, $CDCl_3$) δ 12.37 (s, 1H), 7.83 (s, 1H), 7.49 (t, $J = 7.4$ Hz, 2H), 7.42–7.33 (m, 3H), 4.70 (d, $J = 1.8$ Hz, 2H), 3.92 (t, $J = 5.6$ Hz, 2H), 2.81 (t, $J = 5.7$ Hz, 2H), 1.45 (s, 9H). LC-MS (ESI) m/z 391.0 $[M + H]^+$. Purity 100.0%.

tert-Butyl 6-(3-phenylthioureido)-3,4-dihydro-2H-thieno[2,3-b]pyran-5-carboxylate (39). Using a similar procedure as described for **11** with **2h** (50 mg, 0.20 mmol) and phenyl isothiocyanate (26 mg, 0.20 mmol), white solid (51 mg, 65%). 1H NMR (300 MHz, $CDCl_3$) δ 12.29 (s, 1H), 7.79 (s, 1H), 7.46 (t, $J = 7.5$ Hz, 2H), 7.41–7.30 (m, 3H), 4.21–4.12 (m, 2H), 2.68 (t, $J = 6.4$ Hz, 2H), 1.98 (p, $J = 6.2$ Hz, 2H), 1.44 (s, 9H). LC-MS (ESI) m/z 391.0 $[M + H]^+$. Purity 100.0%.

tert-Butyl 6,6-dimethyl-2-(3-phenylthioureido)-6,7-dihydro-4H-thieno[3,2-c]pyran-3-carboxylate (40). Using a similar procedure as described for **11** with **2i** (50 mg, 0.18 mmol) and phenyl isothiocyanate (24 mg, 0.18 mmol), white solid (47 mg, 62%). 1H NMR (300 MHz, $CDCl_3$) δ 12.36 (s, 1H), 7.87 (s, 1H), 7.48 (t, $J = 7.4$ Hz, 2H), 7.38 (dd, $J = 13.5, 7.1$ Hz, 3H), 4.70 (s, 2H), 2.66 (s, 2H), 1.45 (s, 9H), 1.29 (s, 6H). LC-MS (ESI) m/z 419.1 $[M + H]^+$. Purity 98.1%.

tert-Butyl 6-methyl-2-(3-phenylthioureido)-4,5,6,7-tetrahydrothieno[2,3-c]pyridine-3-carboxylate (42). Using a similar procedure as described for **11** with **2j** (84 mg, 0.31 mmol) and phenyl isothiocyanate (37 mg, 0.31 mmol), light yellow solid (35 mg, 28%). 1H NMR (300 MHz, $DMSO-d_6$) δ 11.90 (s, 1H), 11.02 (s, 1H), 7.47 (d, $J = 8.0$ Hz, 2H), 7.39 (t, $J = 7.6$ Hz, 2H), 7.23

(t, $J = 7.3$ Hz, 1H), 3.40 (s, 2H), 2.76 (s, 2H), 2.59 (t, $J = 5.8$ Hz, 2H), 2.34 (s, 3H), 1.51 (s, 9H).

LC-MS (ESI) m/z 404.1 $[M + H]^+$. Purity 98.9%.

tert-Butyl 6-benzyl-2-(3-phenylthioureido)-4,5,6,7-tetrahydrothieno[2,3-c]pyridine-3-carboxylate (43). Using a similar procedure as described for **11** with **2k** (143 mg, 0.42 mmol) and phenyl isothiocyanate (56 mg, 0.42 mmol), light yellow solid (140 mg, 70%). ^1H NMR (300 MHz, CDCl_3) δ 12.38 (s, 1H), 7.89 (s, 1H), 7.48 (dd, $J = 8.5, 6.8$ Hz, 4H), 7.43–7.33 (m, 6H), 3.96 (s, 2H), 3.80 (s, 2H), 3.01 (s, 4H), 1.44 (s, 9H). LC-MS (ESI) m/z 480.2 $[M + H]^+$. Purity 98.0%.

Ethyl 2-isothiocyanato-4-methyl-4,5,6,7-tetrahydrobenzo[b]thiophene-3-carboxylate (3a). To an ice-cooled suspension of CSCl_2 (0.96 g, 8.37 mmol) and CaCO_3 (0.84 g, 8.37 mmol) in DCM (5 mL) and H_2O (10 mL) was added dropwise a solution of **2a** (2.00 g, 8.37 mmol) in DCM (10 mL). After stirred at room temperature overnight, the mixture was concentrated, diluted with Et_2O , washed with H_2O , brine, and dried over anhydrous Na_2SO_4 . The resulting mixture was purified with silica chromatography (5% EtOAc in hexane) to give **3a** as a white solid (2.09 g, 89%). ^1H NMR (300 MHz, CDCl_3) δ 4.38 (qd, $J = 7.1, 1.9$ Hz, 2H), 3.47–3.32 (m, 3H), 2.77–2.54 (m, 2H), 1.98–1.75 (m, 3H), 1.75–1.61 (m, 2H), 1.43 (t, $J = 7.1$ Hz, 3H), 1.16 (d, $J = 6.8$ Hz, 3H).

tert-Butyl 2-isothiocyanato-4-methyl-4,5,6,7-tetrahydrobenzo[b]thiophene-3-carboxylate (3b). Using a similar procedure as described for **3a** with **2c** (267 mg, 1.00 mmol), and purified with silica chromatography (5% EtOAc in hexane). White solid (374 mg, 70%). ^1H NMR (300 MHz, CDCl_3) δ 3.39–3.28 (m, 1H), 2.74–2.52 (m, 2H), 1.95–1.66 (m, 4H), 1.62 (s, 9H), 1.15 (d, $J = 6.9$ Hz, 3H).

tert-Butyl 2-isothiocyanato-5,7-dihydro-4H-thieno[2,3-c]pyran-3-carboxylate (3c). Using a similar procedure as described for **3a** with **2g** (510 mg, 2.00 mmol), and purified with silica chromatography (10% EtOAc in hexane). Light yellow solid (516 mg, 87%). $^1\text{H NMR}$ (300 MHz, CDCl_3) δ 4.68 (t, $J = 1.8$ Hz, 2H), 3.96 (t, $J = 5.6$ Hz, 2H), 2.91 (ddd, $J = 5.7, 3.9, 1.8$ Hz, 2H), 1.61 (s, 10H).

Ethyl 2-(3-(4-fluorophenyl)thioureido)-4-methyl-4,5,6,7-tetrahydrobenzo[b]thiophene-3-carboxylate (12). A mixture of **3a** (60 mg, 0.21 mmol) and 4-fluoroaniline (24 mg, 0.21 mol) were heated in pyridine (2 mL) at 50°C for 3 h. The solvent was removed by evaporation. MeOH was added to the residue and white solid was precipitated. The mixture was filtered, and the solid was washed by MeOH to give **12** as a white solid. (24 mg, 29%). $^1\text{H NMR}$ (300 MHz, CDCl_3) δ 12.26 (s, 1H), 7.77 (s, 1H), 7.39–7.31 (m, 2H), 7.18 (t, $J = 8.5$ Hz, 2H), 4.27–4.11 (m, 2H), 3.30 (d, $J = 7.3$ Hz, 1H), 2.77–2.52 (m, 2H), 1.92–1.67 (m, 4H), 1.31 (t, $J = 7.1$ Hz, 3H), 1.13 (d, $J = 6.8$ Hz, 3H). LC-MS (ESI) m/z 393.0 $[\text{M} + \text{H}]^+$. Purity 96.6%.

Ethyl 2-(3-(4-methoxyphenyl)thioureido)-4-methyl-4,5,6,7-tetrahydrobenzo[b]thiophene-3-carboxylate (13). Using a similar procedure as described for **12** with **3a** (50 mg, 0.18 mmol) and 4-methoxyaniline (22 mg, 0.18 mmol), white solid (33 mg, 58%). $^1\text{H NMR}$ (300 MHz, CDCl_3) δ 12.09 (s, 1H), 7.71 (s, 1H), 7.26 (d, $J = 2.3$ Hz, 2H), 7.05–6.97 (m, 2H), 4.26–4.04 (m, 2H), 3.88 (s, 3H), 3.29 (d, $J = 7.6$ Hz, 1H), 2.76–2.54 (m, 2H), 1.96 – 1.68 (m, 4H), 1.28 (t, $J = 7.1$ Hz, 3H), 1.12 (d, $J = 6.8$ Hz, 3H). LC-MS (ESI) m/z 405.0 $[\text{M} + \text{H}]^+$. Purity 95.3%.

Ethyl 4-methyl-2-(3-(4-(trifluoromethoxy)phenyl)thioureido)-4,5,6,7-tetrahydrobenzo[b]thiophene-3-carboxylate (14). Using a similar procedure as described for **12** with **3a** (30 mg, 0.11 mmol) and 4-trifluoromethoxyaniline (19 mg, 0.11 mmol), white solid (43 mg, 86%). $^1\text{H NMR}$ (300 MHz, CDCl_3) δ 12.37 (s, 1H), 7.82 (s, 1H), 7.45–7.30 (m, 4H), 4.26–

4.07 (m, 2H), 3.31 (s, 1H), 2.80–2.51 (m, 2H), 1.97–1.66 (m, 4H), 1.31 (t, $J = 7.1$ Hz, 3H), 1.13 (d, $J = 6.8$ Hz, 3H). LC-MS (ESI) m/z 459.1 $[M + H]^+$. Purity 97.6%.

Ethyl 2-(3-(4-(dimethylamino)phenyl)thioureido)-4-methyl-4,5,6,7-tetrahydrobenzo[b]thiophene-3-carboxylate (15). Using a similar procedure as described for **12** with **3a** (50 mg, 0.18 mmol) and *N,N*-dimethyl-*p*-phenylenediamine (24 mg, 0.18 mmol), white solid (70 mg, 93%). ^1H NMR (300 MHz, CDCl_3) δ 11.96 (s, 1H), 7.70 (s, 1H), 7.22 (d, $J = 8.5$ Hz, 2H), 6.86 (s, 2H), 4.13 (p, $J = 6.9$ Hz, 2H), 3.30 (d, $J = 7.6$ Hz, 1H), 3.04 (s, 6H), 2.75–2.49 (m, 2H), 1.94–1.67 (m, 4H), 1.26 (t, $J = 7.1$ Hz, 3H), 1.12 (d, $J = 6.8$ Hz, 3H). LC-MS (ESI) m/z 418.2 $[M + H]^+$. Purity 99.4%.

Ethyl 2-(3-(4-(tert-butyl)phenyl)thioureido)-4-methyl-4,5,6,7-tetrahydrobenzo[b]thiophene-3-carboxylate (16). Using a similar procedure as described for **12** with **3a** (50 mg, 0.18 mmol) and 4-(*tert*-butyl)aniline (27 mg, 0.18 mmol), white solid (30 mg, 39%). ^1H NMR (300 MHz, Chloroform-*d*) δ 12.09 (s, 1H), 7.75 (s, 1H), 7.55–7.48 (m, 2H), 7.26 (d, $J = 2.1$ Hz, 2H), 4.10 (p, $J = 7.2$ Hz, 2H), 3.30 (s, 1H), 2.75–2.53 (m, 2H), 1.92–1.64 (m, 4H), 1.38 (s, 9H), 1.25 (t, $J = 7.1$ Hz, 3H), 1.12 (d, $J = 6.8$ Hz, 3H). LC-MS (ESI) m/z 431.1 $[M + H]^+$. Purity 97.9%.

Ethyl 2-(3-(2,2-difluorobenzo[d][1,3]dioxol-5-yl)thioureido)-4-methyl-4,5,6,7-tetrahydrobenzo[b]thiophene-3-carboxylate (17). Using a similar procedure as described for **12** with **3a** (50 mg, 0.18 mmol) and 2,2-difluorobenzo[d][1,3]dioxol-5-amine (31 mg, 0.18 mmol), white solid (52 mg, 65%). ^1H NMR (300 MHz, $\text{DMSO-}d_6$) δ 11.95 (s, 1H), 11.09 (s, 1H), 7.66 (s, 1H), 7.45 (d, $J = 8.6$ Hz, 1H), 7.20 (d, $J = 10.5$ Hz, 1H), 4.27 (dd, $J = 13.3, 6.9$ Hz, 2H), 3.30 (s, 1H), 2.74–2.53 (m, 2H), 1.70 (d, $J = 33.4$ Hz, 4H), 1.30 (t, $J = 7.1$ Hz, 3H), 1.12 (d, $J = 6.7$ Hz, 3H). LC-MS (ESI) m/z 455.0 $[M + H]^+$. Purity 99.2%.

Ethyl 2-(3-(3,4-dimethoxyphenyl)thioureido)-4-methyl-4,5,6,7-tetrahydrobenzo[b]thiophene-3-carboxylate (18). Using a similar procedure as described for **12** with **3a** (50 mg, 0.18 mmol) and

3,4-dimethoxyaniline (27 mg, 0.18 mmol), white solid (67 mg, 86%). ^1H NMR (300 MHz, CDCl_3) δ 12.23 (s, 1H), 7.81 (s, 1H), 6.92 (d, $J = 10.1$ Hz, 3H), 4.25–4.10 (m, 2H), 3.93 (d, $J = 9.9$ Hz, 6H), 3.30 (s, 1H), 2.80–2.58 (m, 2H), 1.75 (d, $J = 39.4$ Hz, 4H), 1.29 (t, $J = 7.1$ Hz, 3H), 1.12 (d, $J = 6.8$ Hz, 3H). LC-MS (ESI) m/z 435.0 $[\text{M} + \text{H}]^+$. Purity 96.7%.

Ethyl 4-methyl-2-(3-(4-(trifluoromethyl)phenyl)thioureido)-4,5,6,7-tetrahydrobenzo[b]thiophene-3-carboxylate (19). Using a similar procedure as described for **12** with **3a** (50 mg, 0.18 mmol) and 4-(trifluoromethyl)aniline (29 mg, 0.18 mmol), light yellow solid (43 mg, 55%). ^1H NMR (300 MHz, CDCl_3) δ 12.58 (s, 1H), 7.91 (s, 1H), 7.72 (d, $J = 8.4$ Hz, 2H), 7.51 (d, $J = 8.3$ Hz, 2H), 4.24 (qq, $J = 10.9, 7.1$ Hz, 2H), 3.33 (s, 1H), 2.78–2.55 (m, 2H), 1.84 (td, $J = 14.0, 13.4, 6.9$ Hz, 4H), 1.34 (t, $J = 7.1$ Hz, 3H), 1.16 (d, $J = 6.8$ Hz, 3H). LC-MS (ESI) m/z 443.1 $[\text{M} + \text{H}]^+$. Purity 99.0%.

Ethyl 2-(3-(4-aminophenyl)thioureido)-4-methyl-4,5,6,7-tetrahydrobenzo[b]thiophene-3-carboxylate (20). Using a similar procedure as described for **12** with **3a** (30 mg, 0.11 mmol) and benzene-1,4-diamine (12 mg, 0.11 mmol), white solid (31 mg, 72%). ^1H NMR (300 MHz, CDCl_3) δ 11.97 (s, 1H), 7.65 (s, 1H), 7.11 (d, $J = 8.3$ Hz, 2H), 6.76 (d, $J = 8.2$ Hz, 2H), 4.26–4.06 (m, 2H), 3.87 (s, 2H), 3.31 (s, 1H), 2.78–2.52 (m, 2H), 1.93–1.56 (m, 4H), 1.28 (t, $J = 7.1$ Hz, 3H), 1.12 (d, $J = 6.7$ Hz, 3H). LC-MS (ESI) m/z 390.0 $[\text{M} + \text{H}]^+$. Purity 99.3%.

Ethyl 2-(3-(4-hydroxyphenyl)thioureido)-4-methyl-4,5,6,7-tetrahydrobenzo[b]thiophene-3-carboxylate (21). Using a similar procedure as described for **12** with **3a** (50 mg, 0.18 mmol) and 4-aminophenol (20 mg, 0.18 mmol), white solid (62 mg, 88%). ^1H NMR (300 MHz, CDCl_3) δ 12.04 (s, 1H), 7.70 (s, 1H), 7.20 (d, $J = 8.7$ Hz, 2H), 6.90 (d, $J = 8.7$ Hz, 2H), 4.25–4.09 (m, 2H), 3.30 (s, 1H), 2.64 (tdd, $J = 16.5, 12.9, 5.5$ Hz, 2H), 1.94–1.60 (m, 4H), 1.29 (t, $J = 7.1$ Hz, 3H), 1.12 (d, $J = 6.8$ Hz, 3H). LC-MS (ESI) m/z 391.0 $[\text{M} + \text{H}]^+$. Purity 99.5%.

Ethyl 2-(3-(2-hydroxyphenyl)thioureido)-4-methyl-4,5,6,7-tetrahydrobenzo[b]thiophene-3-carboxylate (22). Using a similar procedure as described for **12** with **3a** (50 mg, 0.18 mmol) and 4-aminophenol (27 mg, 0.18 mmol), white solid (58 mg, 82%). ¹H NMR (300 MHz, CDCl₃) δ 12.22 (s, 1H), 7.67 (s, 1H), 7.31 (d, *J* = 14.3 Hz, 2H), 7.15–6.95 (m, 2H), 4.31–4.09 (m, 2H), 3.30 (d, *J* = 6.4 Hz, 1H), 2.79–2.48 (m, 2H), 1.97–1.58 (m, 4H), 1.31 (t, *J* = 7.1 Hz, 3H), 1.13 (d, *J* = 6.8 Hz, 3H). LC-MS (ESI) *m/z* 391.1 [M + H]⁺. Purity 96.6%.

Ethyl 2-(3-(2-fluorophenyl)thioureido)-4-methyl-4,5,6,7-tetrahydrobenzo[b]thiophene-3-carboxylate (23). Using a similar procedure as described for **12** with **3a** (50 mg, 0.18 mmol) and 4-aminophenol (20 mg, 0.18 mmol), white solid (39 mg, 55%). ¹H NMR (300 MHz, CDCl₃) δ 12.41 (s, 1H), 7.66–7.52 (m, 2H), 7.41–7.31 (m, 1H), 7.28–7.18 (m, 2H), 4.21 (qq, *J* = 10.8, 7.1 Hz, 2H), 3.31 (d, *J* = 7.4 Hz, 1H), 2.77–2.54 (m, 2H), 1.93–1.65 (m, 4H), 1.32 (t, *J* = 7.1 Hz, 3H), 1.14 (d, *J* = 6.8 Hz, 3H). LC-MS (ESI) *m/z* 393.0 [M + H]⁺. Purity 98.0%.

Ethyl 2-(3-(3-methoxyphenyl)thioureido)-4-methyl-4,5,6,7-tetrahydrobenzo[b]thiophene-3-carboxylate (24). Using a similar procedure as described for **12** with **3a** (30 mg, 0.11 mmol) and 4-aminophenol (14 mg, 0.11 mmol), white solid (27 mg, 61%). ¹H NMR (300 MHz, CDCl₃) δ 12.35 (s, 1H), 7.84 (s, 1H), 7.38 (t, *J* = 8.2 Hz, 1H), 6.96–6.87 (m, 3H), 4.18 (dtt, *J* = 13.5, 7.1, 3.6 Hz, 2H), 3.85 (s, 3H), 3.31 (d, *J* = 6.8 Hz, 1H), 2.77–2.52 (m, 2H), 1.95–1.58 (m, 4H), 1.30 (t, *J* = 7.1 Hz, 3H), 1.13 (d, *J* = 6.8 Hz, 3H). LC-MS (ESI) *m/z* 405.1 [M + H]⁺. Purity 96.6%.

Ethyl 2-(3-benzylthioureido)-4-methyl-4,5,6,7-tetrahydrobenzo[b]thiophene-3-carboxylate (25). Using a similar procedure as described for **12** with **3a** (50 mg, 0.18 mmol) and 4-aminophenol (19 mg, 0.18 mmol), white solid (68 mg, 97%). ¹H NMR (300 MHz, CDCl₃) δ 12.34 (s, 1H), 7.45–7.30 (m, 5H), 6.40 (s, 1H), 4.73 (s, 2H), 4.45–4.24 (m, 2H), 3.34 (t, *J* = 6.4 Hz, 1H), 2.78–

2.52 (m, 2H), 1.96–1.65 (m, 4H), 1.40 (t, $J = 7.1$ Hz, 3H), 1.18 (d, $J = 6.8$ Hz, 3H). LC-MS (ESI) m/z 389.1 $[M + H]^+$. Purity 97.9%.

tert-Butyl 2-(3-(3-methoxyphenyl)thioureido)-4-methyl-4,5,6,7-tetrahydrobenzo[b]thiophene-3-carboxylate (44). Using a similar procedure as described for **12** with **3b** (40 mg, 0.13 mmol) and 3-methoxyaniline (16 mg, 0.13 mmol), white solid (32 mg, 57%). ^1H NMR (300 MHz, CDCl_3) δ 12.56 (s, 1H), 7.78 (s, 1H), 7.41–7.33 (m, 1H), 6.91 (q, $J = 5.5, 4.8$ Hz, 3H), 3.84 (s, 3H), 3.27 (d, $J = 6.1$ Hz, 1H), 2.76–2.58 (m, 2H), 1.95–1.74 (m, 4H), 1.48 (s, 9H), 1.13 (d, $J = 6.8$ Hz, 3H). LC-MS (ESI) m/z 433.1 $[M + H]^+$. Purity 99.3%.

tert-Butyl 4-methyl-2-(3-(4-(trifluoromethoxy)phenyl)thioureido)-4,5,6,7-tetrahydrobenzo[b]thiophene-3-carboxylate (45). Using a similar procedure as described for **12** with **3b** (40 mg, 0.13 mmol) and 4-trifluoromethoxyaniline (23 mg, 0.13 mmol), white solid (33 mg, 52%). ^1H NMR (300 MHz, CDCl_3) δ 12.56 (s, 1H), 7.74 (s, 1H), 7.41 (d, $J = 8.6$ Hz, 2H), 7.33 (d, $J = 8.6$ Hz, 2H), 3.27 (s, 1H), 2.68 (s, 2H), 1.82 (s, 4H), 1.47 (s, 9H), 1.13 (d, $J = 6.8$ Hz, 3H). LC-MS (ESI) m/z 487.1 $[M + H]^+$. Purity 97.9%.

tert-Butyl 2-(3-(4-(tert-butoxy)phenyl)thioureido)-4-methyl-4,5,6,7-tetrahydrobenzo[b]thiophene-3-carboxylate (46). Using a similar procedure as described for **12** with **3b** (40 mg, 0.13 mmol) and 4-*tert*-butoxyaniline (21 mg, 0.13 mmol), white solid (31 mg, 50%). ^1H NMR (300 MHz, $\text{DMSO-}d_6$) δ 11.97 (s, 1H), 10.67 (s, 1H), 7.30 (d, $J = 8.4$ Hz, 2H), 7.02 (d, $J = 8.6$ Hz, 2H), 3.24 (s, 1H), 2.64 (d, $J = 16.2$ Hz, 2H), 1.68 (d, $J = 36.3$ Hz, 4H), 1.47 (s, 9H), 1.32 (s, 9H), 1.10 (d, $J = 6.7$ Hz, 3H). LC-MS (ESI) m/z 475.2 $[M + H]^+$. Purity 98.9%.

tert-Butyl 4-methyl-2-(3-(4-phenoxyphenyl)thioureido)-4,5,6,7-tetrahydrobenzo[b]thiophene-3-carboxylate (47). Using a similar procedure as described for **12** with **3b** (40 mg, 0.13 mmol) and 4-phenoxyaniline (24 mg, 0.13 mmol), white solid (54 mg, 84%). ^1H NMR (300 MHz, DMSO-

d6) δ 12.02 (s, 1H), 10.80 (s, 1H), 7.41 (t, $J = 9.3$ Hz, 4H), 7.16 (t, $J = 7.4$ Hz, 1H), 7.05 (dd, $J = 8.9, 2.6$ Hz, 4H), 3.26 (s, 1H), 2.61 (t, $J = 19.2$ Hz, 2H), 1.75 (s, 4H), 1.52 (s, 9H), 1.12 (d, $J = 6.7$ Hz, 3H). LC-MS (ESI) m/z 495.2 [M + H]⁺. Purity 99.2%.

tert-Butyl 4-methyl-2-(3-(4-(4-methylpiperazin-1-yl)phenyl)thioureido)-4,5,6,7-tetrahydrobenzo[*b*]thiophene-3-carboxylate (**48**). Using a similar procedure as described for **12** with **3b** (40 mg, 0.13 mmol) and 4-(4-methylpiperazin-1-yl)aniline (25 mg, 0.13 mmol), white solid (46 mg, 71%). ¹H NMR (300 MHz, CDCl₃) δ 12.29 (s, 1H), 7.74 (s, 1H), 7.22 (d, $J = 8.6$ Hz, 2H), 6.98 (d, $J = 8.6$ Hz, 2H), 3.35 (t, $J = 5.0$ Hz, 4H), 3.25 (s, 1H), 2.75 (s, 4H), 2.68 – 2.56 (m, 2H), 2.48 (s, 3H), 1.95 – 1.57 (m, 4H), 1.45 (s, 9H), 1.11 (d, $J = 6.8$ Hz, 3H). LC-MS (ESI) m/z 501.2 [M + H]⁺. Purity 100.0%.

tert-Butyl 2-(3-(3,4-dimethoxyphenyl)thioureido)-4-methyl-4,5,6,7-tetrahydrobenzo[*b*]thiophene-3-carboxylate (**49**). Using a similar procedure as described for **12** with **3b** (40 mg, 0.13 mmol) and 3,4-dimethoxyaniline (20 mg, 0.13 mmol), white solid (45 mg, 75%). ¹H NMR (300 MHz, DMSO-*d6*) δ 11.98 (s, 1H), 10.66 (s, 1H), 7.07–6.95 (m, 2H), 6.92 (s, 1H), 3.77 (s, 3H), 3.74 (s, 3H), 3.24 (s, 1H), 2.71–2.52 (d, $J = 16.8$ Hz, 2H), 1.83–1.58 (d, $J = 35.4$ Hz, 4H), 1.48 (s, 9H), 1.10 (d, $J = 6.7$ Hz, 3H). LC-MS (ESI) m/z 463.2 [M + H]⁺. Purity 99.5%.

tert-Butyl 2-(3-(2,2-difluorobenzo[*d*][1,3]dioxol-5-yl)thioureido)-4-methyl-4,5,6,7-tetrahydrobenzo[*b*]thiophene-3-carboxylate (**50**). Using a similar procedure as described for **12** with **3b** (40 mg, 0.13 mmol) and 2,2-difluorobenzo[*d*][1,3]dioxol-5-amine (22 mg, 0.13 mmol), white solid (44 mg, 70%). ¹H NMR (300 MHz, CDCl₃) δ 12.54 (s, 1H), 7.22 – 7.13 (m, 2H), 7.07 (dd, $J = 8.4, 2.1$ Hz, 1H), 3.33–3.20 (m, 1H), 2.78–2.56 (m, 2H), 1.95–1.65 (m, 4H), 1.47 (s, 9H), 1.13 (d, $J = 6.8$ Hz, 3H). LC-MS (ESI) m/z 483.2 [M + H]⁺. Purity 99.4%.

tert-Butyl 2-(3-phenylthioureido)-5,7-dihydro-4H-thieno[2,3-c]pyran-3-carboxylate (52). Using a similar procedure as described for **12** with **3c** (40 mg, 0.13 mmol) and 4-fluoroaniline (15 mg, 0.13 mmol), white solid (30 mg, 57%). ¹H NMR (300 MHz, DMSO-*d*₆) δ 11.90 (s, 1H), 11.05 (s, 1H), 7.50 (dd, *J* = 8.8, 5.0 Hz, 2H), 7.24 (t, *J* = 8.8 Hz, 2H), 4.60 (s, 2H), 3.83 (t, *J* = 5.6 Hz, 2H), 2.76 (t, *J* = 5.8 Hz, 2H), 1.52 (s, 9H). ¹³C NMR (101 MHz, CDCl₃) δ 176.69, 165.88, 163.24, 160.78, 150.34, 131.83, 131.80, 128.58, 128.50, 128.34, 124.00, 116.91, 116.69, 113.83, 82.27, 65.11, 64.69, 28.24, 27.10. LC-MS (ESI) *m/z* 409.2 [M + H]⁺. Purity 100.0%.

tert-Butyl 2-(3-(4-(trifluoromethoxy)phenyl)thioureido)-5,7-dihydro-4H-thieno[2,3-c]pyran-3-carboxylate (53). Using a similar procedure as described for **12** with **3c** (50 mg, 0.17 mmol) and 4-trifluoromethoxyaniline (30 mg, 0.17 mmol), white solid (41 mg, 51%). ¹H NMR (300 MHz, DMSO-*d*₆) δ 11.97 (s, 1H), 11.19 (s, 1H), 7.63 (d, *J* = 8.8 Hz, 2H), 7.40 (d, *J* = 8.5 Hz, 2H), 4.61 (s, 2H), 3.83 (t, *J* = 5.6 Hz, 2H), 2.76 (t, *J* = 5.6 Hz, 2H), 1.52 (s, 9H). LC-MS (ESI) *m/z* 475.2 [M + H]⁺. Purity 99.3%.

tert-Butyl 2-(3-(3,4-dimethoxyphenyl)thioureido)-5,7-dihydro-4H-thieno[2,3-c]pyran-3-carboxylate (54). Using a similar procedure as described for **12** with **3c** (50 mg, 0.17 mmol) and 3,4-dimethoxyaniline (26 mg, 0.17 mmol), white solid (71 mg, 93%). ¹H NMR (300 MHz, DMSO-*d*₆) δ 11.90 (s, 1H), 10.81 (s, 1H), 7.05 (s, 1H), 6.97 (t, *J* = 9.1 Hz, 2H), 4.60 (s, 2H), 3.82 (t, *J* = 5.5 Hz, 2H), 3.77 (s, 3H), 3.74 (s, 3H), 2.74 (t, *J* = 5.5 Hz, 2H), 1.48 (s, 9H). LC-MS (ESI) *m/z* 451.1 [M + H]⁺. Purity 99.4%.

(S)-tert-Butyl 2-(3-(1-phenylethyl)thioureido)-5,7-dihydro-4H-thieno[2,3-c]pyran-3-carboxylate (55). Using a similar procedure as described for **12** with **3c** (40 mg, 0.13 mmol) and (*S*)-1-phenylethylamine (16 mg, 0.13 mmol), white solid (42 mg, 78%). ¹H NMR (300 MHz, DMSO) δ 11.56 (s, 1H), 9.94 (s, 1H), 7.41–7.30 (m, 4H), 7.29–7.21 (m, 1H), 5.50–5.33 (m, 1H), 4.57 (s,

2H), 3.81 (t, $J = 5.6$ Hz, 2H), 2.75 (t, $J = 5.5$ Hz, 2H), 1.56 (s, 9H), 1.48 (d, $J = 7.0$ Hz, 3H). LC-MS (ESI) m/z 419.2 $[M + H]^+$. Purity 100.0%.

(R)-tert-Butyl 2-(3-(1-phenylethyl)thioureido)-5,7-dihydro-4H-thieno[2,3-c]pyran-3-carboxylate (56). Using a similar procedure as described for **12** with **3c** (40 mg, 0.13 mmol) and (*R*)-1-phenylethylamine (16 mg, 0.13 mmol), white solid (44 mg, 81%). ^1H NMR (300 MHz, DMSO-*d*₆) δ 11.56 (s, 1H), 9.94 (s, 1H), 7.41–7.29 (m, 4H), 7.29 – 7.19 (m, 1H), 4.57 (s, 2H), 3.81 (t, $J = 5.5$ Hz, 2H), 2.75 (t, $J = 5.0$ Hz, 2H), 1.56 (s, 9H), 1.48 (d, $J = 6.9$ Hz, 3H). LC-MS (ESI) m/z 419.1 $[M + H]^+$. ^{13}C NMR (101 MHz, DMSO) δ 176.93, 165.62, 151.38, 144.00, 128.77, 127.94, 127.36, 126.78, 123.23, 112.00, 81.91, 64.79, 64.30, 53.78, 28.44, 27.38, 22.26. Purity 100.0%.

6-((9H-Fluoren-9-yl)methyl) 3-tert-butyl 2-amino-4,5-dihydrothieno[2,3-c]pyridine-3,6(7H)-dicarboxylate (4). To a solution of **2l** (93 mg, 0.37 mmol) and Na_2CO_3 (105 mg, 0.99 mmol) in dioxane (4 mL) and H_2O (0.4 mL) was added 9-fluorenylmethoxycarbonyl chloride (86 mg, 0.33 mmol). The mixture was stirred at room temperature overnight. The mixture was diluted by EtOAc and water, and the organic layer was washed with brine, dried over Na_2SO_4 , filtered and concentrated. The residue was purified with silica chromatography (10% EtOAc in hexane) to give **4** as a white solid (100 mg, 57%). ^1H NMR (300 MHz, CDCl_3) δ 7.78 (t, $J = 6.8$ Hz, 4H), 7.67–7.54 (m, 2H), 7.42 (s, 2H), 7.33 (t, $J = 7.2$ Hz, 2H), 6.00 (s, 2H), 4.52–4.38 (m, 4H), 4.30 (s, 1H), 3.69 (t, $J = 5.9$ Hz, 2H), 2.80 (t, $J = 5.8$ Hz, 2H), 1.58 (d, $J = 3.7$ Hz, 9H). LC-MS (ESI) m/z 477.1 $[M + H]^+$.

tert-Butyl 2-(3-phenylthioureido)-4,5,6,7-tetrahydrothieno[2,3-c]pyridine-3-carboxylate (41). A mixture of **4** (100 mg, 0.21 mmol) and phenyl isothiocyanate (25 mg, 0.21 mmol) were heated in pyridine (3 mL) at 60°C for 5 h. The solvent was removed by evaporation. MeOH was added to the residue and white solid was generated. The mixture was filtered, and the solid was washed by

MeOH to give 6-((9*H*-fluoren-9-yl)methyl) 3-*tert*-butyl 2-(3-phenylthioureido)-4,5-dihydrothieno[2,3-*c*]pyridine-3,6(7*H*)-dicarboxylate as a white solid. It was dissolved in DMF (0.8 mL), and piperidine (0.2 mL) was added dropwise. The mixture was stirred at room temperature for 4 h and concentrated under vacuum. The residue obtained was purified with prep-HPLC to give **41** as a white solid (20mg, 24%). ¹H NMR (300 MHz, CDCl₃) δ 12.41 (s, 1H), 7.97 (s, 1H), 7.55 – 7.45 (m, 2H), 7.39 (dd, *J* = 14.6, 7.3 Hz, 3H), 4.27 (s, 2H), 3.42 (t, *J* = 6.6 Hz, 2H), 3.14 – 3.06 (m, 2H), 1.45 (s, 9H). LC-MS (ESI) *m/z* 431.2 [M + CH₃CN + H]⁺. Purity 97.2%.

Ethyl 2-((tert-butoxycarbonyl)amino)-4-methyl-4,5,6,7-tetrahydrobenzo[b]thiophene-3-carboxylate (5). To a solution of **2a** (1.00 g, 4.18 mmol) and DMAP (51 mg, 0.42 mmol) in dioxane (15 mL) was added (Boc)₂O (1.82 g, 8.37 mmol). The mixture was stirred at 40 °C overnight and concentrated. The residue was purified by silica chromatography (10% EtOAc in hexane) to give a colorless gel (1.32 g, 93%). ¹H NMR (300 MHz, CDCl₃) δ 4.32–4.13 (m, 2H), 3.45–3.30 (m, 1H), 2.78–2.54 (m, 2H), 1.96–1.57 (m, 4H), 1.41 (s, 9H), 1.30 (t, *J* = 7.1 Hz, 3H), 1.14 (d, *J* = 6.6 Hz, 3H).

2-((tert-Butoxycarbonyl)amino)-4-methyl-4,5,6,7-tetrahydrobenzo[b]thiophene-3-carboxylic acid (6). To a solution of **5** (1.30 g, 3.83 mmol) in a mixed solvent of THF (5 mL), MeOH (5 mL) and H₂O (2.5 mL) was added NaOH (767 mg, 19.2 mmol). The mixture was stirred at 80 °C for 2 h, and the organic solvent was removed by evaporation. The resulting suspension was diluted by H₂O, and neutralized by 1N HCl aqueous solution. White solid precipitated and was filtered, washed by H₂O to give the product (700 mg, 59%). ¹H NMR (300 MHz, MeOD) δ 3.44–3.32 (m, 1H), 2.73–2.52 (m, 2H), 1.99–1.65 (m, 4H), 1.54 (s, 9H), 1.19 (d, *J* = 6.7 Hz, 3H).

tert-Butyl (4-methyl-3-(methylcarbamoyl)-4,5,6,7-tetrahydrobenzo[b]thiophen-2-yl)carbamate (7a). To a solution of **6** (300 mg, 1.40 mmol), methylamine hydrochloride (190 mg, 2.80 mmol) and HATU (640 mg, 1.70 mmol) in DMF (15 mL) was added DIEA (540 mg, 4.20 mmol) and stirred at room temperature overnight. The mixture was diluted with EtOAc, washed with H₂O for 2 times, and washed by brine. The solution obtained was dried over anhydrous Na₂SO₄ and purified by silica chromatography (10% EtOAc in hexane) to give **7a** as a white solid (200 mg, 44%). ¹H NMR (300 MHz, CDCl₃) δ 10.69 (s, 1H), 5.99 (s, 1H), 2.97 (d, J = 4.8 Hz, 3H), 2.96–2.86 (m, 1H), 2.72–2.54 (m, 2H), 2.00–1.59 (m, 4H), 1.50 (s, 9H), 1.21 (d, J = 6.9 Hz, 3H).

N,4-Dimethyl-2-(3-phenylthioureido)-4,5,6,7-tetrahydrobenzo[b]thiophene-3-carboxamide (33). **7a** (23 mg, 0.071 mmol) was dissolved in a solution of HCl in dioxane (4M, 0.5 mL) and the mixture was stirred at room temperature for 3 h. The white precipitates generated were filtered and washed by Et₂O to give 2-amino-*N,4*-dimethyl-4,5,6,7-tetrahydrobenzo[b]thiophene-3-carboxamide as a HCl salt. It was dissolved in pyridine (0.5 mL) and phenyl isothiocyanate was added. The mixture was heated at 60 °C for 40 min and then concentrated. The residue was purified by silica chromatography (30% EtOAc in hexane) to give **33** as a white solid (16 mg, 62%). ¹H NMR (300 MHz, MeOD) δ 7.49–7.36 (m, 4H), 7.33–7.21 (m, 1H), 3.21–3.06 (m, 1H), 2.83 (s, 3H), 2.66 (q, J = 5.7 Hz, 2H), 2.04–1.74 (m, 3H), 1.65–1.53 (m, 1H), 1.10 (d, J = 6.8 Hz, 3H). LC-MS (ESI) m/z 360.1 [M + H]⁺. Purity 94.6%.

tert-Butyl (3-(benzylcarbamoyl)-4-methyl-4,5,6,7-tetrahydrobenzo[b]thiophen-2-yl)carbamate (7b). To a solution of **6** (60 mg, 0.19 mmol), benzylamine (24 mg, 0.23 mmol) and HATU (87 mg, 0.23 mmol) in DMF (2 mL) was added DIEA (74 mg, 0.57 mmol) and stirred at room temperature overnight. The mixture was diluted with EtOAc, washed with H₂O for 2 times, and washed by brine. The solution obtained was dried over anhydrous Na₂SO₄ and purified by silica

chromatography (20% EtOAc in hexane) to give **7b** as a white solid (52 mg, 68%). ¹H NMR (300 MHz, CDCl₃) δ 10.79 (s, 1H), 7.41–7.27 (m, 5H), 6.29 (s, 1H), 4.63 (qd, *J* = 14.8, 5.5 Hz, 2H), 2.95–2.82 (m, 1H), 2.73–2.50 (m, 2H), 2.00–1.59 (m, 4H), 1.52 (s, 9H), 1.18 (d, *J* = 6.9 Hz, 3H). LC-MS (ESI) *m/z* 401.1 [M + H]⁺.

N-Benzyl-4-methyl-2-(3-phenylthioureido)-4,5,6,7-tetrahydrobenzo[*b*]thiophene-3-carboxamide (**35**). **7b** (52 mg, 0.13 mmol) was dissolved in a solution of HCl in dioxane (4M, 0.5 mL) and the mixture was stirred at room temperature for 3 h. The precipitates generated was then filtered and washed by dioxane to give 2-amino-*N*-benzyl-4-methyl-4,5,6,7-tetrahydrobenzo[*b*]thiophene-3-carboxamide as a HCl salt. It was dissolved in pyridine (1.0 mL) and phenyl isothiocyanate was added. The mixture was heated at 60 °C for 40 min and concentrated. The residue was purified by silica chromatography (33% EtOAc in hexane) to give **35** as a white solid (25 mg, 45%). ¹H NMR (300 MHz, CDCl₃) δ 7.48–7.29 (m, 8H), 7.24 (d, *J* = 7.3 Hz, 2H), 4.63–4.34 (m, 2H), 2.97 (s, 1H), 2.77–2.48 (m, 2H), 1.98–1.53 (m, 4H), 1.13 (d, *J* = 6.9 Hz, 3H). LC-MS (ESI) *m/z* 436.2 [M + H]⁺. Purity 95.8%.

2-Cyano-*N*-phenylacetamide (**8**). To a solution of 2-cyanoacetic acid (200 mg, 2.35 mmol), EDCI (544 mg, 2.82 mmol) and HOBt (381 mg, 2.82 mmol) in DMF (2 mL) was added Et₃N (712 mg, 7.05 mmol) and stirred at room temperature overnight. The mixture was diluted with EtOAc, washed with H₂O and brine. The solution obtained was dried over anhydrous Na₂SO₄ and purified by silica chromatography (10% EtOAc in hexane) to give **8** as a white solid (172 mg, 46%). ¹H NMR (300 MHz, CDCl₃) δ 7.71 (s, 1H), 7.53 (d, *J* = 8.0 Hz, 2H), 7.40 (t, *J* = 7.7 Hz, 2H), 7.22 (s, 1H), 3.59 (s, 2H).

2-Cyano-2-(2-methylcyclohexylidene)-*N*-phenylacetamide (**9a**). To a solution of **8** (86 mg, 0.54 mmol) and 2-methylcyclohexanone (60 mg, 0.54 mmol) in toluene (2 mL) was added NH₄OAc

(21 mg, 0.27 mmol) and AcOH (26 mg, 0.43 mmol) and stirred at 80 °C for 5 h. The mixture was diluted with EtOAc, washed with H₂O and brine. The solution obtained was dried over anhydrous Na₂SO₄ and purified by silica chromatography (20% EtOAc in hexane) to give **9a** as a white solid (31 mg, 23%), which was directly used in the next step.

2-Cyano-N-phenyl-2-(tetrahydro-4H-pyran-4-ylidene)acetamide (9b). Using a similar procedure as described for **9a** with **8** (560 mg, 3.50 mmol) and tetrahydro-4H-pyran-4-one (350 mg, 3.50 mmol) and purified with silica chromatography (20% EtOAc in hexane) to give **9b** as a yellow solid (355 mg, 42%), which was directly used in the next step.

2-Amino-4-methyl-N-phenyl-4,5,6,7-tetrahydrobenzo[b]thiophene-3-carboxamide (10a). A solution of sulfur (4 mg, 0.12 mmol), **9a** (31 mg, 0.12 mmol) and morpholine (11 mg, 0.12 mmol) in EtOH was heated at 70 °C for 20 h and concentrated. The residue was purified with silica chromatography (20% EtOAc in hexane) to give **10** as a white solid (10 mg, 28%). ¹H NMR (300 MHz, CDCl₃) δ 7.73 (s, 1H), 7.59–7.52 (m, 2H), 7.42–7.32 (m, 2H), 7.13 (t, *J* = 7.4 Hz, 1H), 3.14–2.99 (m, 1H), 2.58 (t, *J* = 6.0 Hz, 2H), 2.07–1.61 (m, 4H), 1.30 (d, *J* = 6.9 Hz, 3H). LC-MS (ESI) *m/z* 287.0 [M + H]⁺.

2-Amino-N-phenyl-4,7-dihydro-5H-thieno[2,3-c]pyran-3-carboxamide (10b). Using a similar procedure as described for **10a** with **9b** (317 mg, 1.31 mmol) and purified with silica chromatography (20% EtOAc in hexane) to give **10** as a light yellow solid (147 mg, 41%). ¹H NMR (300 MHz, CDCl₃) δ 7.54 (d, *J* = 8.3 Hz, 2H), 7.37 (t, *J* = 7.7 Hz, 2H), 7.14 (t, *J* = 7.3 Hz, 1H), 4.65 (s, 2H), 4.01 (t, *J* = 5.4 Hz, 2H), 2.91 (t, *J* = 5.5 Hz, 2H). LC-MS (ESI) *m/z* 275.2 [M + H]⁺.

4-Methyl-N-phenyl-2-(3-phenylthioureido)-4,5,6,7-tetrahydrobenzo[b]thiophene-3-carboxamide (34). A mixture of **10a** (10 mg, 0.035 mol) and phenyl isothiocyanate (4.7 mg, 0.035 mol) were

heated in pyridine (0.5 mL) at 60 °C for 5 h. The solvent was removed by evaporation. The residue was purified with prep-HPLC to give **34** as a white solid. (4 mg, 27%). ¹H NMR (300 MHz, CDCl₃) δ 11.11 (s, 1H), 8.21 (s, 1H), 7.98 (s, 1H), 7.49 (dd, *J* = 12.7, 7.7 Hz, 4H), 7.42–7.30 (m, 5H), 7.18 (d, *J* = 7.3 Hz, 1H), 3.17–3.01 (m, 1H), 2.81–2.63 (m, 2H), 1.99–1.62 (m, 4H), 1.26 (d, *J* = 6.9 Hz, 3H). LC-MS (ESI) *m/z* 422.1 [M + H]⁺. Purity 100.0%.

*2-(3-(4-Fluorophenyl)thioureido)-N-phenyl-4,7-dihydro-5H-thieno[2,3-*c*]pyran-3-carboxamide (51)*. Using a similar procedure as described for **34** with **10b** (50 mg, 0.18 mmol) and 4-fluorophenyl isothiocyanate (28 mg, 0.18 mmol) and purified with flash chromatography (30% EtOAc in hexane) to give **51** as a light brown solid (10 mg, 13%). ¹H NMR (400 MHz, DMSO) δ 11.04 (s, 1H), 10.79 (s, 1H), 9.72 (s, 1H), 7.66 (d, *J* = 7.4 Hz, 2H), 7.49 (dd, *J* = 9.0, 5.0 Hz, 2H), 7.41–7.31 (m, 2H), 7.20 (t, *J* = 8.8 Hz, 2H), 7.12 (t, *J* = 7.4 Hz, 1H), 4.70 (d, *J* = 1.8 Hz, 2H), 3.86 (t, *J* = 5.4 Hz, 2H), 2.84 (t, *J* = 4.6 Hz, 2H). LC-MS (ESI) *m/z* 428.0 [M + H]⁺. Purity 100.0%.

Cell culture

TangoTM CXCR2-bla and CXCR4-bla U2OS cells were purchased from Invitrogen (Carlsbad, CA, USA) and grown in McCoy5A supplemented with 10% dialyzed FBS, zeocin (200 μg·mL⁻¹), hygromycin (50 μg·mL⁻¹), geneticin (100 μg·mL⁻¹), 1 mM sodium pyruvate, 0.1 mM non-essential amino acids and 25 mM HEPES. OVCAR8 cells were cultured in RPMI 1640 medium (Gibco) supplemented with 10% FBS (Gibco). All the cells were grown at 37 °C in a humidified atmosphere of 5% CO₂. All of the cell lines used were maintained in culture under 35 passages and tested regularly for Mycoplasma contamination using Plasmoguard Test (InvivoGen, San Diego, CA).

CXCR2/4 Tango assay

The inhibition of stimulus mediated CXCR2/4 β -arrestin recruitment was assayed by TangoTM assay (Thermo Fisher) as described previously.¹² CXCR2/4-bla (beta-lactamase) U2OS cells were genetically modified to stably overexpress CXCR2 or CXCR4 linked to a TEV protease site and a GAL4-VP16 transcription factor, via a reporter-gene system. These cells also stably express a β -arrestin/TEV protease fusion protein and a β -lactamase reporter gene. Upon corresponding stimulus (CXCL8 or SDF1- α) binding and resulting CXCR2 or CXCR4 activation, the β -arrestin/TEV fusion protein is recruited to the receptor and cleaves the peptide linker that links CXCR2/4 to the GAL4-VP16 transcription factor. GAL4-VP16 now can enter the nucleus and promote the transcription of the β -lactamase gene. β -Lactamase activity is detected using a FRET-based fluorescence assay with CCF4-AM, a β -lactamase FRET substrate. CCF4-AM is cleaved in the presence of β -lactamase. The cleaved substrate excites at 409 nm and emits at 460 nm. In the absence of β -lactamase, CCF4-AM will not be cleaved and excites at 409 nm and emits at 540 nm. Thus, the activation of CXCR2/4 is directly correlated with the amount of cleaved β -lactamase substrate.

In each assay, CXCR2 or CXCR4-bla U2OS cells were seeded (11000/well) in 384-well tissue culture plates for 24 h in DMEM supplemented with 1% dialysis FBS. Cells were pretreated with various concentrations of inhibitors for 30 min prior to the addition of 12 nM of CXCL8 or 60 nM of SDF1- α and incubated for 5 h at 37 °C. Then β -Lactamase substrate (CCF4-AM dye) was loaded for 2 h, and plates were read on Clario Star microplate reader at 409 nm excitation and 464/530 nm emissions. Percent inhibition was calculated using the following formulas:

$$\text{Ratio} = \text{cleaved (405/464)}/\text{uncleaved (409/530)}$$

$$\% \text{ inhibition} = [1 - ((\text{compound treated-unstimulated control})/(\text{CXCL8/SDF stimulated-unstimulated control}))] \times 100\%$$

Calcium Flux

293T-CXCR2-GFP cells were seeded at 30000 cells/well in 384-well black plates with clear bottom plates in growth medium. The next day, the cells were loaded with Fluo-4 NW and probenecid according to the manufacturer's protocol (Invitrogen). Briefly, the dye mixture included in the kit was diluted with 10 mL of assay buffer and 100 μ L of probenecid (25 mM final concentration). The growth medium was replaced with 25 μ L of the dye mixture, and the cells were incubated at 37 °C for 30 min and at room temperature for 30 min (protected from light). To detect the calcium flux induced by the TOTP compounds or SB265610, 5 \times compound was added to each well, and the fluorescence signal was detected immediately on the Clario Star plate reader with 490 nm excitation and 535 nm emission filters. To detect CXCL8-stimulated calcium flux, 5 \times TOTP compounds and 5 \times CXCL8 (5 μ L) were added to each well, and the fluorescence signal was detected immediately on the Clario Star plate reader with 490 nm excitation and 535 nm emission filters. The fluorescence signal was normalized to the baseline signal prior to any stimulation.

Wound-Healing Assay

CXCR2-bla U2OS Tango cells were seeded in 96-well plates (35000 cells/well) in DMEM supplemented with 1% FBS overnight. The following day, a single scratch was introduced using a 200 μ L sterile pipet tip. Cells were subsequently treated with compounds at various concentrations and recombinant CXCL8 (100 nM) for 24 h. Cells were fixed with 100% methanol for 15 min and stained with Giemsa stain for 1 h. Each well was imaged on BD Pathway 435 bioimager with transmitted light. The data reported is a representative of at least two independent experiments.

Cyclic AMP Assay

293T-CXCR2-GFP-p22F cells were seeded at 30000 cells/well in CO₂-independent media (Invitrogen) supplemented with 10% FBS overnight in white 384-well plates. The following day, cells were incubated with 1% cAMP reagent (Promega) for 2 h at 37 °C. Cells were pretreated with various concentrations of compounds or SB265610 for 10 min, then CXCL8 (50 nM) for another 10 min prior to forskolin (50 µM) stimulation until max signal was reached. Luminescence signals were detected using the Clario Star microplate reader (PerkinElmer, Waltham, MA).

Immunoblot

293T-CXCR2-GFP cells were seeded into 6-well microtiter plates for 5×10^5 cells per well, and allowed to attach overnight before treated with appropriate compounds at indicated concentrations for appropriate time. Then, cells were lysated with RIPA buffer in the presence of protease and phosphatase inhibitors. The cells were collected, centrifuged and the pellet was discarded. Protein concentration of whole-cell lysate in the supernatant was determined by BCA protein assay kit (Thermo Scientific). Proteins were resolved on 10% SDS/PAGE and electrotransferred to transfer membrane (Immobilon®-FL). After incubating in blocking buffer (5% nonfat dry milk in TBST) at room temperature for 1 h, membranes were probed with primary antibody (1:500-1:1000) in blocking buffer overnight at 4 °C, and then washed 3 times for 5 min with TBST, followed by incubation in anti-rabbit or anti-mouse secondary antibody in blocking buffer (Dylight 800 4× PEG conjugated; Thermo Scientific; 1:75000) at room temperature for 1 h. The membranes were imaged by Odyssey® CLx Imaging System after washing 3 times with TBST. Antibodies to the following targets were used: p-ERK1/2 (Cell signaling 4370S), p-JNK (Cell signaling 9251), p-cJUN (Santa Cruz Biotechnology, sc-53182), p-p38 (Santa Cruz Biotechnology, sc-166182).

Colony formation assay

Cells were seeded in 96-well tissue culture plates at a density of 300 cells per well. After overnight attachment, cells were treated with compounds at appropriate concentrations. After 7-10 days, when colonies had formed in the DMSO-treated wells, cells were stained with a 0.05% crystal violet solution for 30 min, and then washed with ddH₂O to remove excess stain. Plates were imaged using Odyssey Imaging Systems (LI-COR Biosciences) after overnight drying.

AUTHOR INFORMATION

Corresponding Author

*Phone, (734)647-2732; E-mail, neamati@med.umich.edu. Address: North Campus Research Complex, Building 520, 1600 Huron Parkway, Ann Arbor, Michigan 48109, United States.

Author Contributions

∇D.X. and W.C. contributed equally.

ACKNOWLEDGMENT

We thank Dr. Yibin Xu and Dr. Xinde Chen for critical reading of the manuscript. GPCR screening data was generously provided by the National Institute of Mental Health's Psychoactive Drug Screening Program, Contract # HHSN-271-2018-00023-C (NIMH PDSP). The NIMH PDSP is Directed by Bryan L. Roth at the University of North Carolina at Chapel Hill and Project Officer Jamie Driscoll at NIMH, Bethesda MD, USA. For experimental details please refer to the PDSP web site <https://pdsp.unc.edu/ims/investigator/web/>.

ABBREVIATIONS

(Boc)₂O, di-*tert*-butyl dicarbonate; CaCO₃, calcium carbonate; cAMP, cyclic adenosine monophosphate; COPD, chronic obstructive pulmonary disorder; CXCL8, chemokine (C-X-C motif) ligand 8; CXCR2, chemokine (C-X-C motif) receptor 2; DCM, dichloromethane; DIEA, diisopropylethylamine; DMAP, 4-Dimethylaminopyridine; DMF, *N,N*-dimethylformamide; ERK, extracellular signal-regulated kinase; EtOH, ethanol; EtOAc, ethyl acetate; EDCI, 1-ethyl-3-(3-(dimethylamino)propyl)-carbodiimide; Fmoc-Cl, Fluorenylmethyloxycarbonyl chloride; HATU, (1-[Bis(dimethylamino)methylene]-1*H*-1,2,3-triazolo[4,5-*b*]pyridinium 3-oxid hexafluorophosphate; HCl, hydrogen chloride; hERG, the human ether-à-go-go-related gene; HOBt, hydroxybenzotriazole; K₂CO₃, potassium carbonate; LCMS, liquid chromatography-mass spectrometry; MAPK, mitogen-activated protein kinases; MgSO₄, magnesium sulfate; Na₂CO₃, sodium carbonate; NaOH, sodium hydroxide; SAR, structure-activity relationship, SDF-1, stromal cell-derived factor 1; TFA, trifluoroacetic acid; THF, tetrahydrofuran; TUTP, 2-thioureidothiophene-3-carboxylate.

REFERENCES

- (1) Olson, T. S.; Ley, K. Chemokines and chemokine receptors in leukocyte trafficking. *Am. J. Physiol.-Regul. Integr. Comp. Physiol.* **2002**, *283*, R7-R28.
- (2) Ha, H.; Debnath, B.; Neamati, N. Role of the CXCL8-CXCR1/2 axis in cancer and inflammatory diseases. *Theranostics* **2017**, *7*, 1543-1588.
- (3) Russo, R. C.; Garcia, C. C.; Teixeira, M. M.; Amaral, F. A. The CXCL8/IL-8 chemokine family and its receptors in inflammatory diseases. *Expert Rev. Clin. Immunol.* **2014**, *10*, 593-619.
- (4) Jaffer, T.; Ma, D. Q. The emerging role of chemokine receptor CXCR2 in cancer progression. *Transl. Cancer Res.* **2016**, *5*, S616-S628.

- (5) Zhao, J. K.; Ou, B. C.; Feng, H.; Wang, P. X. Z.; Yin, S.; Zhu, C. C.; Wang, S. J.; Chen, C.; Zheng, M. H.; Zong, Y. P.; Sun, J.; Lu, A. G. Overexpression of CXCR2 predicts poor prognosis in patients with colorectal cancer. *Oncotarget* **2017**, *8*, 28442-28454.
- (6) Zhang, H.; Ye, Y. L.; Li, M. X.; Ye, S. B.; Huang, W. R.; Cai, T. T.; He, J.; Peng, J. Y.; Duan, T. H.; Cui, J.; Zhang, X. S.; Zhou, F. J.; Wang, R. F.; Li, J. CXCL2/MIF-CXCR2 signaling promotes the recruitment of myeloid-derived suppressor cells and is correlated with prognosis in bladder cancer. *Oncogene* **2017**, *36*, 2095-2104.
- (7) Li, L.; Xu, L.; Yan, J.; Zhen, Z. J.; Ji, Y.; Liu, C. Q.; Lau, W. Y.; Zheng, L. M.; Xu, J. CXCR2-CXCL1 axis is correlated with neutrophil infiltration and predicts a poor prognosis in hepatocellular carcinoma. *J. Exp. Clin. Cancer Res.* **2015**, *34*, 129.
- (8) Han, L.; Jiang, B.; Wu, H.; Wang, X. D.; Tang, X. J.; Huang, J. F.; Zhu, J. High expression of CXCR2 is associated with tumorigenesis, progression, and prognosis of laryngeal squamous cell carcinoma. *Med. Oncol.* **2012**, *29*, 2466-2472.
- (9) Wilson, C. R.; Wilson, T. R.; Johnston, P. G.; Longley, D. B.; Waugh, D. J. Interleukin-8/CXCR2 signaling plays an important role in conferring resistance of prostate cancer cells to chemotherapy. *Mol. Cancer Ther.* **2007**, *6*, 3394s-3395s.
- (10) Wilson, C.; Purcell, C.; Seaton, A.; Oladipo, O.; Maxwell, P. J.; O'Sullivan, J. M.; Wilson, R. H.; Johnston, P. G.; Waugh, D. J. Chemotherapy-induced CXC-chemokine/CXC-chemokine receptor signaling in metastatic prostate cancer cells confers resistance to oxaliplatin through potentiation of nuclear factor-kappa B transcription and evasion of apoptosis. *J. Pharmacol. Exp. Ther.* **2008**, *327*, 746-759.

- (11) Sharma, B.; Nawandar, D. M.; Nannuru, K. C.; Varney, M. L.; Singh, R. K. Targeting CXCR2 enhances chemotherapeutic response, inhibits mammary tumor growth, angiogenesis, and lung metastasis. *Mol. Cancer Ther.* **2013**, *12*, 799-808.
- (12) Ha, H.; Debnath, B.; Odde, S.; Bensman, T.; Ho, H.; Beringer, P. M.; Neamati, N. Discovery of novel CXCR2 inhibitors using ligand-based pharmacophore models. *J. Chem Inf. Model.* **2015**, *55*, 1720-1738.
- (13) Che, J. X.; Wang, Z. L.; Sheng, H. C.; Huang, F.; Dong, X. W.; Hu, Y. H.; Xie, X.; Hu, Y. Z. Ligand-based pharmacophore model for the discovery of novel CXCR2 antagonists as anti-cancer metastatic agents. *Roy Soc Open Sci* **2018**, *5*.
- (14) Che, J. X.; Wang, Z. L.; Dong, X. W.; Hu, Y. H.; Xie, X.; Hu, Y. Z. Bicyclo[2.2.1]heptane containing N,N-diarylsquaramide CXCR2 selective antagonists as anti-cancer metastasis agents. *Rsc Adv* **2018**, *8*, 11061-11069.
- (15) Cesarini, S.; Spallarossa, A.; Ranise, A.; Bruno, O.; Arduino, N.; Bertolotto, M.; Dallegri, F.; Tognolini, M.; Gobetti, T.; Barocelli, E. 6-Amino-4-oxo-1,3-diphenyl-2-thioxo-1,2,3,4-tetrahydropyrimidine-5-carbonyl derivatives as a new class of potent inhibitors of Interleukin-8-induced neutrophil chemotaxis. *Biorg. Med. Chem.* **2009**, *17*, 3580-3587.
- (16) Dwyer, M. P.; Yu, Y. N. CXCR2 receptor antagonists: a medicinal chemistry perspective. *Curr. Top. Med. Chem.* **2014**, *14*, 1590-1605.
- (17) White, J. R.; Lee, J. M.; Young, P. R.; Hertzberg, R. P.; Jurewicz, A. J.; Chaikin, M. A.; Widdowson, K.; Foley, J. J.; Martin, L. D.; Griswold, D. E.; Sarau, H. M. Identification of a potent, selective non-peptide CXCR2 antagonist that inhibits interleukin-8-induced neutrophil migration. *J. Biol. Chem.* **1998**, *273*, 10095-10098.

- (18) Moss, R. B.; Mistry, S. J.; Konstan, M. W.; Pilewski, J. M.; Kerem, E.; Tal-Singer, R.; Lazaar, A. L.; Investigators, C. Safety and early treatment effects of the CXCR2 antagonist SB-656933 in patients with cystic fibrosis. *J Cyst Fibros* **2013**, *12*, 241-248.
- (19) Lazaar, A. L.; Sweeney, L. E.; MacDonald, A. J.; Alexis, N. E.; Chen, C.; Tal-Singer, R. SB-656933, a novel CXCR2 selective antagonist, inhibits ex vivo neutrophil activation and ozone-induced airway inflammation in humans. *Br. J. Clin. Pharmacol.* **2011**, *72*, 282-293.
- (20) Lu, H. F.; Yang, T.; Xu, Z. M.; Lin, X. C.; Ding, Q.; Zhang, Y. T.; Cai, X.; Dong, K.; Gong, S.; Zhang, W.; Patel, M.; Copley, R. C. B.; Xiang, J. N.; Guan, X. M.; Wren, P.; Ren, F. Discovery of novel 1-cyclopentenyl-3-phenylureas as selective, brain penetrant, and orally bioavailable CXCR2 antagonists. *J. Med. Chem.* **2018**, *61*, 2518-2532.
- (21) Singh, S.; Sadanandam, A.; Nannuru, K. C.; Varney, M. L.; Mayer-Ezell, R.; Bond, R.; Singh, R. K. Small-molecule antagonists for CXCR2 and CXCR1 inhibit human melanoma growth by decreasing tumor cell proliferation, survival, and angiogenesis. *Clin. Cancer. Res.* **2009**, *15*, 2380-2386.
- (22) Steele, C. W.; Karim, S. A.; Leach, J. D. G.; Bailey, P.; Upstill-Goddard, R.; Rishi, L.; Foth, M.; Bryson, S.; McDaid, K.; Wilson, Z.; Eberlein, C.; Candido, J. B.; Clarke, M.; Nixon, C.; Connelly, J.; Jamieson, N.; Carter, C. R.; Balkwill, F.; Chang, D. K.; Evans, T. R. J.; Strathdee, D.; Biankin, A. V.; Nibbs, R. J. B.; Barry, S. T.; Sansom, O. J.; Morton, J. P. CXCR2 inhibition profoundly suppresses metastases and augments immunotherapy in pancreatic ductal adenocarcinoma. *Cancer Cell* **2016**, *29*, 832-845.
- (23) Nair, P.; Gaga, M.; Zervas, E.; Alagha, K.; Hargreave, F. E.; O'Byrne, P. M.; Stryszak, P.; Gann, L.; Sadeh, J.; Chanez, P.; Investigators, S. Safety and efficacy of a CXCR2 antagonist in

patients with severe asthma and sputum neutrophils: a randomized, placebo-controlled clinical trial. *Clin. Exp. Allergy* **2012**, *42*, 1097-1103.

(24) Allegretti, M.; Bertini, R.; Cesta, M. C.; Bizzarri, C.; Di Bitondo, R.; Di Cioccio, V.; Galliera, E.; Berdini, V.; Topai, A.; Zampella, G.; Russo, V.; Di Bello, N.; Nano, G.; Nicolini, L.; Locati, M.; Fantucci, P.; Florio, S.; Colotta, F. 2-Arylpropionic CXC chemokine receptor 1 (CXCR1) ligands as novel noncompetitive CXCL8 inhibitors. *J. Med. Chem.* **2005**, *48*, 4312-4331.

(25) Virtala, R.; Ekman, A. K.; Jansson, L.; Westin, U.; Cardell, L. O. Airway inflammation evaluated in a human nasal lipopolysaccharide challenge model by investigating the effect of a CXCR2 inhibitor. *Clin. Exp. Allergy* **2012**, *42*, 590-596.

(26) Sun, L.; Clavijo, P. E.; Robbins, Y.; Patel, P.; Friedman, J.; Greene, S.; Das, R.; Silvin, C.; Van Waes, C.; Horn, L. A.; Schlom, J.; Palena, C.; Maeda, D.; Zebala, J.; Allen, C. T. Inhibiting myeloid-derived suppressor cell trafficking enhances T cell immunotherapy. *Jci Insight* **2019**, *4*, e126853.

(27) Lu, X.; Horner, J. W.; Paul, E.; Shang, X. Y.; Troncoso, P.; Deng, P. N.; Jiang, S.; Chang, Q.; Spring, D. J.; Sharma, P.; Zebala, J. A.; Maeda, D. Y.; Wang, Y. A.; DePinho, R. A. Effective combinatorial immunotherapy for castration-resistant prostate cancer. *Nature* **2017**, *543*, 728-732.

(28) Ha, H.; Neamati, N. Pyrimidine-based compounds modulate CXCR2-mediated signaling and receptor turnover. *Mol. Pharm.* **2014**, *11*, 2431-2441.

(29) Ishikawa, M.; Hashimoto, Y. Improvement in aqueous solubility in small molecule drug discovery programs by disruption of molecular planarity and symmetry. *J. Med. Chem.* **2011**, *54*, 1539-1554.

- (30) Waring, M. J. Lipophilicity in drug discovery. *Expert. Opin. Drug Discov.* **2010**, *5*, 235-248.
- (31) Wu, C. H.; Coumar, M. S.; Chu, C. Y.; Lin, W. H.; Chen, Y. R.; Chen, C. T.; Shiao, H. Y.; Rafi, S.; Wang, S. Y.; Hsu, H.; Chen, C. H.; Chang, C. Y.; Chang, T. Y.; Lien, T. W.; Fang, M. Y.; Yeh, K. C.; Chen, C. P.; Yeh, T. K.; Hsieh, S. H.; Hsu, J. T. A.; Liao, C. C.; Chao, Y. S.; Hsieh, H. P. Design and synthesis of tetrahydropyridothieno[2,3-d]pyrimidine scaffold based epidermal growth factor receptor (EGFR) kinase inhibitors: the role of side chain chirality and michael acceptor group for maximal potency. *J. Med. Chem.* **2010**, *53*, 7316-7326.
- (32) Pisal, M. M.; Nawale, L. U.; Patil, M. D.; Bhansali, S. G.; Gajbhiye, J. M.; Sarkar, D.; Chavan, S. P.; Borate, H. B. Hybrids of thienopyrimidinones and thiouracils as anti-tubercular agents: SAR and docking studies. *Eur. J. Med. Chem.* **2017**, *127*, 459-469.
- (33) Pochetti, G.; Montanari, R.; Gege, C.; Chevrier, C.; Taveras, A. G.; Mazza, F. Extra binding region induced by non-zinc chelating inhibitors into the S-1 ' subsite of matrix metalloproteinase 8 (MMP-8). *J. Med. Chem.* **2009**, *52*, 1040-1049.
- (34) Truong, E. C.; Phuan, P. W.; Reggi, A. L.; Ferrera, L.; Galiotta, L. J. V.; Levy, S. E.; Moises, A. C.; Cil, O.; Diez-Cecilia, E.; Lee, S. J.; Verlanan, A. S.; Anderson, M. O. Substituted 2-acylaminoalkylthiophene-3-carboxylic acid arylamides as inhibitors of the calcium-activated chloride channel transmembrane protein 16A (TMEM16A). *J. Med. Chem.* **2017**, *60*, 4626-4635.
- (35) Lefkowitz, R. J.; Whalen, E. J. beta-arrestins: traffic cops of cell signaling. *Curr. Opin. Cell Biol.* **2004**, *16*, 162-168.
- (36) Violin, J. D.; Lefkowitz, R. J. beta-arrestin-biased ligands at seven-transmembrane receptors. *Trends Pharmacol. Sci.* **2007**, *28*, 416-422.

- (37) Raghuwanshi, S. K.; Su, Y. J.; Singh, V.; Haynes, K.; Richmond, A.; Richardson, R. M. The chemokine receptors CXCR1 and CXCR2 couple to distinct G protein-coupled receptor kinases to mediate and regulate leukocyte functions. *J. Immunol.* **2012**, *189*, 2824-2832.
- (38) Teicher, B. A.; Fricker, S. P. Cxcl12 (Sdf-1)/Cxcr4 Pathway in Cancer. *Clin. Cancer. Res.* **2010**, *16*, 2927-2931.
- (39) Dogra, S.; Sona, C.; Kumar, A.; Yadav, P. N. Tango assay for ligand-induced GPCR-beta-arrestin2 interaction: application in drug discovery. *Methods Cell Biol.* **2016**, *132*, 233-254.
- (40) Bradley, M. E.; Bond, M. E.; Manini, J.; Brown, Z.; Charlton, S. J. SB265610 is an allosteric, inverse agonist at the human CXCR2 receptor. *Br. J. Pharmacol.* **2009**, *158*, 328-338.
- (41) Ha, H.; Bensman, T.; Ho, H.; Beringer, P. M.; Neamati, N. A novel phenylcyclohex - 1 - enecarbothioamide derivative inhibits CXCL8 - mediated chemotaxis through selective regulation of CXCR2 - mediated signalling. *Br. J. Pharmacol.* **2014**, *171*, 1551-1565.
- (42) Addison, C. L.; Daniel, T. O.; Burdick, M. D.; Liu, H.; Ehlert, J. E.; Xue, Y. Y.; Buechi, L.; Walz, A.; Richmond, A.; Strieter, R. M. The CXC chemokine receptor 2, CXCR2, is the putative receptor for ELR+ CXC chemokine-induced angiogenic activity. *J. Immunol.* **2000**, *165*, 5269-5277.
- (43) Ning, Y.; Manegold, P. C.; Hong, Y. K.; Zhang, W.; Pohl, A.; Lutje, G.; Winder, T.; Yang, D. Y.; LaBonte, M. J.; Wilson, P. M.; Ladner, R. D.; Lenz, H. J. Interleukin-8 is associated with proliferation, migration, angiogenesis and chemosensitivity in vitro and in vivo in colon cancer cell line models. *Int. J. Cancer* **2011**, *128*, 2038-2049.
- (44) Matte, I.; Lane, D.; Laplante, C.; Rancourt, C.; Piché, A. Profiling of cytokines in human epithelial ovarian cancer ascites. *Am. J. Cancer Res.* **2012**, *2*, 566-580.

- (45) Wang, Y.; Xu, R. C.; Zhang, X. L.; Niu, X. L.; Qu, Y.; Li, L. Z.; Meng, X. Y. Interleukin-8 secretion by ovarian cancer cells increases anchorage-independent growth, proliferation, angiogenic potential, adhesion and invasion. *Cytokine* **2012**, *59*, 145-155.
- (46) Devapatla, B.; Sharma, A.; Woo, S. CXCR2 inhibition combined with sorafenib improved antitumor and antiangiogenic response in preclinical models of ovarian cancer. *PLoS one* **2015**, *10*, e0139237.
- (47) Salchow, K.; Bond, M. E.; Evans, S. C.; Press, N. J.; Charlton, S. J.; Hunt, P. A.; Bradley, M. E. A common intracellular allosteric binding site for antagonists of the CXCR2 receptor. *Br. J. Pharmacol.* **2010**, *159*, 1429-1439.
- (48) Ha, H. L.; Bensman, T.; Ho, H.; Beringer, P. M.; Neamati, N. A novel phenylcyclohex-1-enecarbothioamide derivative inhibits CXCL8-mediated chemotaxis through selective regulation of CXCR2-mediated signalling. *Br. J. Pharmacol.* **2014**, *171*, 1551-1565.
- (49) Reiter, E.; Ahn, S.; Shukla, A. K.; Lefkowitz, R. J. Molecular mechanism of beta-arrestin-biased agonism at seven-transmembrane receptors. *Annu. Rev. Pharmacol. Toxicol.* **2012**, *52*, 179-197.
- (50) Rajagopal, S.; Rajagopal, K.; Lefkowitz, R. J. Teaching old receptors new tricks: biasing seven-transmembrane receptors. *Nat. Rev. Drug Discov.* **2010**, *9*, 373-386.
- (51) Balabanian, K.; Lagane, B.; Pablos, J. L.; Laurent, L.; Planchenault, T.; Verola, O.; Lebbe, C.; Kerob, D.; Dupuy, A.; Hermine, O.; Nicolas, J. F.; Latger-Cannard, W.; Bensoussan, D.; Bordigoni, P.; Baleux, F.; Le Deist, F.; Virelizier, J. L.; Arenzana-Seisdedos, F.; Bachelier, F. WHIM4 syndromes with different genetic anomalies are accounted for by impaired CXCR4 desensitization to CXCL12. *Blood* **2005**, *105*, 2449-2457.

Journal Pre-proof

Highlights

TUTP compounds were identified as novel CXCR2 antagonists through scaffold-hopping strategy

TUTP compounds are selective for CXCR2 among over 50 other GPCRs

TUTP compounds inhibited CXCL8-mediated β -arrestin recruitment and the phosphorylation of ERK1/2

Combination of TUTP compounds (**56**, **52** or **37**) with doxorubicin show synergistic cytotoxicity in human SKOV3 ovarian cancer cells

Declaration of interests

The authors declare that they have no known competing financial interests or personal relationships that could have appeared to influence the work reported in this paper.

The authors declare the following financial interests/personal relationships which may be considered as potential competing interests:

Journal Pre-proof